

Cosmology with mirror dark matter I: linear evolution of perturbations

Paolo Ciarcelluti

*Dipartimento di Fisica, Università di L'Aquila, 67010 Coppito AQ, and
INFN, Laboratori Nazionali del Gran Sasso, 67010 Assergi AQ, Italy
E-mail: ciarcelluti@lngs.infn.it*

Abstract

This is the first paper of a series devoted to the study of the cosmological implications of the parallel mirror world with the same microphysics as the ordinary one, but having smaller temperature, with a limit set by the BBN constraints. The difference in temperature of the ordinary and mirror sectors generates shifts in the key epochs for structure formation, which proceeds in the mirror sector under different conditions. We consider adiabatic scalar primordial perturbations as an input and analyze the trends of all the relevant scales for structure formation (Jeans length and mass, Silk scale, horizon scale) for both ordinary and mirror sectors, comparing them with the CDM case. These scales are functions of the fundamental parameters of the theory (the temperature of the mirror plasma and the amount of mirror baryonic matter), and in particular they are influenced by the difference between the cosmological key epochs in the two sectors. Then we used a numerical code to compute the evolution in linear regime of density perturbations for all the components of a Mirror Universe: ordinary baryons and photons, mirror baryons and photons, and possibly cold dark matter. We analyzed the evolution of the perturbations for different values of mirror temperature and baryonic density, and obtained that for $x = T'/T$ less than a typical value x_{eq} , for which the mirror baryon-photon decoupling happens before the matter-radiation equality, mirror baryons are equivalent to the CDM for the linear structure formation process. Indeed, the smaller the value of x , the closer mirror dark matter resembles standard cold dark matter during the linear regime.

1 Introduction

The present cosmological observations strongly support the main predictions of the inflationary scenario: first, the Universe is flat, with the total energy density very close to the critical $\Omega_0 \approx 1$, and second, primordial density perturbations have nearly flat spectrum, with the scalar spectral index $n \approx 1$. The non-relativistic matter gives only a small fraction of the present energy density, about $\Omega_m \simeq 0.25$, while the rest is attributed to the vacuum energy (cosmological term or dark energy) $\Omega_\Lambda \simeq 0.75$. The fact that Ω_m and Ω_Λ are of the same order gives rise to the so called cosmological coincidence problem: why we live in an epoch when $\rho_m \sim \rho_\Lambda$, if in the early Universe one had $\rho_m \gg \rho_\Lambda$ and in the late Universe one would expect $\rho_m \ll \rho_\Lambda$? The answer can be only related to an anthropic principle: the matter and vacuum energy densities scale differently with the expansion of the Universe, $\rho_m \propto a^{-3}$ and $\rho_\Lambda \propto \text{const.}$, hence they have to coincide at some moment, and we are just happy to be here. Moreover, for substantially larger ρ_Λ no galaxies could be formed and thus there would not be anyone to ask this question.

On the other hand, the matter in the Universe has two components, visible and dark: $\Omega_m = \Omega_b + \Omega_d$. The visible matter consists of baryons with $\Omega_b \approx 0.04$, while the dark

matter with $\Omega_d \approx 0.2$ is constituted by some hypothetic particle species very weakly interacting with the observable matter. It is a tantalizing question why the visible and dark components have so close energy densities? Clearly, the ratio ρ_d/ρ_b does not depend on time as far as with the expansion of the Universe both ρ_b and ρ_d scale as $\propto a^{-3}$.

In view of the standard cosmological paradigm, there is no good reason for having $\Omega_d \sim \Omega_b$, as far as the visible and dark components have different origins. The density of the visible matter is $\rho_b = M_N n_b$, where $M_N \simeq 1$ GeV is the nucleon mass, and n_b is the baryon number density of the Universe. The latter should be produced in a very early Universe by some baryogenesis mechanism, which is presumably related to some B and CP-violating physics at very high energies. The baryon number per photon $\eta = n_b/n_\gamma$ is very small. Observational data on the primordial abundances of light elements and the recent results on the cosmic microwave background radiation (CMB) anisotropies nicely converge to the value $\eta \approx 6 \times 10^{-10}$.

As for dark matter, it is presumably constituted by some cold relics with mass M and number density n_d , and $\rho_d = M n_d$. The most popular candidate for cold dark matter (CDM) is provided by the lightest supersymmetric particle (LSP) with $M_{LSP} \sim 1$ TeV, and its number density n_{LSP} is fixed by its annihilation cross-section. Hence $\rho_b \sim \rho_{LSP}$ requires that $n_b/n_{LSP} \sim M_{LSP}/M_N$ and the origin of such a conspiracy between four independent parameters is unclear: the value M_N is fixed by the QCD scale while M_{LSP} is related to the supersymmetry breaking scale, n_b is determined by B and CP violating properties of the particle theory at very high energies whereas n_{LSP} strongly depends on the supersymmetry breaking details. Within the parameter space of the MSSM (Minimal Supersymmetric Standard Model) it could vary within several orders of magnitude, and moreover, in either case it has nothing to do with the B and CP violating effects. The situation looks even more obscure if the dark component is related e.g. to the primordial oscillations of a classic axion field, in which case the dark matter particles constituted by axions are superlight, with mass $\ll 1$ eV, but they have a condensate with enormously high number density.

A new sight on the problem of dark matter can be given by the concept of mirror world. This idea was studied in ref. [1] and then its phenomenological and cosmological implications discussed in several later papers. In particular, after its first applications to non-baryonic dark matter [2], the mirror matter hypothesis has attracted a significant interest over the last years and has been invoked in many physical and astrophysical questions: large scale structure of the Universe [3, 4], galactic halo [5], MACHOs [6], gamma ray bursts [7, 8], orthopositronium lifetime [9, 10], interpretation of dark matter detection experiments [11], meteoritic event anomalies [12, 13], close-in extrasolar planets [14], Pioneer spacecraft anomalies [15].

Mirror world can be considered as a hidden sector of particles and interactions which are exactly the same as in our visible world¹, and coupling to our world essentially by gravity. Besides the gravity, the two sectors could communicate by other means. In particular, ordinary photons could have kinetic mixing with mirror photons [17], or ordinary (active) neutrinos could mix with mirror (sterile) neutrinos [18].

If the mirror sector exists, then the Universe along with the ordinary (O) photons, neutrinos, baryons, etc. should contain their mirror (M) partners. One could naively think that due to mirror parity the ordinary and mirror particles should have the same cosmological abundances and hence the O and M sectors should have the same cosmological

¹The mirror parity could be spontaneously broken and the weak interaction scales $\langle\phi\rangle = v$ and $\langle\phi'\rangle = v'$ could be different, which leads to somewhat different particle physics in the mirror sector [16]. In this paper we treat only the simplest case, $v = v'$, in which the mirror sector has exactly the same physics as the ordinary one.

evolution. However, this would be in conflict with the Big Bang nucleosynthesis (BBN) bounds on the effective number of extra light neutrinos, since the mirror photons, electrons and neutrinos would give a contribution to the Hubble expansion rate equivalent to $\Delta N_\nu \simeq 6.14$ [19]. Therefore, even if their microphysics is the same, initial conditions are not the same in both sectors, and in the early Universe the M system should have a lower temperature than ordinary particles. This situation is plausible if the two systems are born with different temperatures (the post-inflationary reheating temperature in the M sector is lower than in the visible one [20]), they interact very weakly, so that they do not come into thermal equilibrium with each other (condition automatically fulfilled if the two worlds communicate only via gravity), and both of them expand adiabatically. So they evolve independently and their temperatures remain different at later stages.

At present, the temperature of ordinary relic photons is $T \approx 2.72$ K, and the mass density of ordinary baryons constitutes about 5% of the critical density. Mirror photons should have smaller temperature $T' < T$, so their number density is $n'_\gamma = x^3 n_\gamma$, where $x = T'/T$.² This ratio is a key parameter in our further considerations since it remains nearly invariant during the expansion of the Universe. The BBN limit on ΔN_ν implies the upper bound $x < 0.64 \Delta N_\nu^{1/4}$. If we assume $\Delta N_\nu \lesssim 1$, we obtain $x \lesssim 0.64$ as a limit for the temperature of the mirror sector [19]. The dependence of x on ΔN_ν is indeed very weak, so even a value $x \lesssim 0.7$ could be compatible with the current experimental status. As for mirror baryons, their number density n'_b can be larger than n_b , and if the ratio $\beta = n'_b/n_b$ is about 5 or so, they could constitute the dark matter of the Universe.

In this view, the mirror world idea could give a new twist to dark matter problem. Once the visible matter is built up by ordinary baryons, then the mirror baryons could constitute dark matter in a natural way. They interact with mirror photons, however they are dark in terms of the ordinary photons. The mass of M baryons is the same as the ordinary one, $M'_N = M_N$, and so we have $\beta = \Omega'_b/\Omega_b$. In addition, as far as the two sectors have the same particle physics, it is natural to think that the M baryon number density n'_b is determined by the baryogenesis mechanism which is similar to the one which fixes the O baryon density n_b . Thus, one could question whether the ratio β could be naturally order 1 or somewhat bigger.

There are several baryogenesis mechanisms as are GUT baryogenesis, leptogenesis, electroweak baryogenesis, etc. At present it is not possible to say definitely which of the known mechanisms is responsible for the observed baryon asymmetry in the ordinary world. However, it is most likely that the baryon asymmetry in the mirror world is produced by the same mechanism and moreover, the properties of the B and CP violation processes are parametrically the same in both cases. But the mirror sector has a lower temperature than ordinary one, and so at epochs relevant for baryogenesis the out-of-equilibrium conditions should be easier fulfilled for the M sector.

In particular, we know that in certain baryogenesis scenarios the M world gets a larger baryon asymmetry than the O sector, and it is pretty plausible that $\beta \gtrsim 1$ [19]. This situation emerges in a particularly appealing way in the leptogenesis scenario due to the lepton number leaking from the O to the M sector which leads to $n'_b \geq n_b$, and can thus explain the near coincidence of visible and dark components in a rather natural way [21].

Given its consistency with all the experimental situation so far, it's important to construct a complete theory of cosmology with mirror dark matter and test this scenario. Thus the aim of this work (described in this paper and the next one of this series, hereafter referred to as Paper 2 [22]) is contained in a question: "is mirror matter still a reliable dark matter candidate?" Its emergence arises also from the astrophysical problems encountered

²From now on all quantities of the mirror sector will be marked by ' to distinguish from the ones belonging to the observable or ordinary world.

by the standard candidate, the cold dark matter (CDM), as for example the central galactic density profiles or the number of small satellites.

In this first paper, we focus on the structure formation theory in linear regime, analyzing the trends of scales in both sectors and comparing them with the CDM case, and finally showing the evolution of perturbations in all the components of a Mirror Universe³ (ordinary and mirror photons and baryons, and possibly CDM). The paper is organized as follows. In section 2 we show that, due to the temperature difference, in mirror sector the key epochs for structure formation occur at different redshifts than in the observable sector. The section 3 analyzes the relevant scales for structure formation (sound speed, Jeans length and mass, Silk mass) as functions of the temperature and the baryonic density of the mirror sector. The main differences with respect to ordinary baryonic and CDM scenarios are also discussed. In section 4 we study the possible mirror scenarios for the growth of primordial perturbations. Section 5 is devoted to the study of the temporal evolution of perturbations in all the ordinary and mirror components. Finally, in section 6 we briefly summarize our findings.

2 Mirror baryons as dark matter

Since it interacts only gravitationally with our ordinary sector, the mirror matter is a *natural dark matter* candidate. At present there are observational evidences that dark matter exists and its density is about 5 times that of ordinary baryons, but in previous section we said that this is not a problem for mirror scenario, because the same microphysics does not imply the same initial conditions in both O and M sectors.

In the most general context, the present energy density contains relativistic (radiation) component Ω_r , non-relativistic (matter) component Ω_m and the vacuum energy density Ω_Λ . According to the inflationary paradigm the Universe should be almost flat, $\Omega_0 = \Omega_m + \Omega_r + \Omega_\Lambda \approx 1$, which well agrees with the results on the CMB anisotropy.

If we consider now a Mirror Universe, i.e. a Universe made of two sectors, Ω_r and Ω_m represent the total amount of radiation and matter of both ordinary and mirror sectors: $\Omega_r = (\Omega_r)_O + (\Omega_r)_M$ and $\Omega_m = (\Omega_m)_O + (\Omega_m)_M$. The two parameters describing the mirror sector are the ratio of the temperatures of two sectors x and the relative amount of mirror baryons compared to the ordinary ones β :

$$x = \frac{T'}{T} \lesssim 0.64 \quad \beta = \frac{\Omega'_b}{\Omega_b} \gtrsim 1. \quad (1)$$

In the above expressions, the first limit comes from the BBN bound on the effective number of extra light neutrinos (see previous section) and the second one from the hypothesis that mirror baryonic contribution to dark matter has cosmological relevance. In the context of our model, as explained in [19], the relativistic fraction is represented by the ordinary and mirror photons and neutrinos, and, using the expression for the ordinary degrees of freedom in a Mirror Universe, $\bar{g}(T) = g_*(T)(1 + x^4)$, and the value of the observable radiation energy density $(\Omega_r)_O h^2 \simeq 4.2 \times 10^{-5}$, it is given by

$$\Omega_r = 4.2 \times 10^{-5} h^{-2} (1 + x^4) \simeq 4.2 \times 10^{-5} h^{-2}, \quad (2)$$

where the contribution of the mirror species, expressed by the additional term x^4 , is negligible in view of the BBN constraint $x < 0.64$. As for the non-relativistic component,

³The expression ‘‘Mirror Universe’’ is clearly misleading, since one could think that there is another Universe, while it is just one, but made of two sectors. Nevertheless, this expression is sometimes used to shortly refer to this scenario.

it contains the O baryon fraction Ω_b and the M baryon fraction $\Omega'_b = \beta\Omega_b$, while the other types of dark matter could also present. Obviously, since mirror parity doubles *all* the ordinary particles, even if they are “dark” (i.e., we are not able to detect them now), whatever the form of dark matter made by some exotic ordinary particles, there will exist a mirror partner made by the mirror counterpart of these particles. In the context of supersymmetry, the CDM component could exist in the form of the lightest supersymmetric particle (LSP). It is interesting to remark that the mass fractions of the ordinary and mirror LSP are related as $\Omega'_{LSP} \simeq x\Omega_{LSP}$. In addition, a significant HDM component Ω_ν could be due to neutrinos with order eV mass. The contribution of the mirror massive neutrinos scales as $\Omega'_\nu = x^3\Omega_\nu$ and thus it is irrelevant. In any case, considering the only CDM component, which is now the preferred candidate, we can combine both the ordinary and mirror components, since their physical effects are exactly the same. Thus we consider a matter composition of the Universe expressed in general by

$$\Omega_m = \Omega_b + \Omega'_b + \Omega_{CDM} = \Omega_b(1 + \beta) + \Omega_{CDM} . \quad (3)$$

The important moments for the structure formation are related to the matter-radiation equality (MRE) epoch and to the plasma recombination and matter-radiation decoupling (MRD) epochs in both sectors. The MRE occurs at the redshift

$$1 + z_{\text{eq}} = \frac{\Omega_m}{\Omega_r} \approx 2.4 \cdot 10^4 \frac{\Omega_m h^2}{1 + x^4} , \quad (4)$$

which is *always smaller than the value obtained for an ordinary Universe*, but approximates it for low x (see fig. 1). If we consider only ordinary and mirror baryons and photons, we find

$$1 + z_{\text{eq}} = \frac{\rho_b(1 + \beta)}{\rho_\gamma(1 + x^4)}(1 + z) = \frac{\rho'_b(1 + \beta^{-1})}{\rho'_\gamma(1 + x^{-4})}(1 + z) , \quad (5)$$

where the baryon and photon densities refer to the redshift z . This implies that, with the addition of a mirror sector, the matter-radiation equality epoch shifts toward earlier times as ⁴

$$1 + z_{\text{eq}} \longrightarrow \frac{(1 + \beta)}{(1 + x^4)} (1 + z_{\text{eq}}) . \quad (6)$$

The MRD, instead, takes place in every sector only after the most of electrons and protons recombine into neutral hydrogen and the free electron number density n_e diminishes, so that the interaction rate of the photons $\Gamma_\gamma = n_e\sigma_T = X_e\eta n_\gamma\sigma_T$ drops below the Hubble expansion rate $H(T)$, where σ_T is the Thomson cross section, $X_e = n_e/n_b$ is the fractional ionization, and $\eta = n_b/n_\gamma$ is the baryon to photon ratio. In condition of chemical equilibrium, X_e is given by the Saha equation, which for $X_e \ll 1$ reads

$$X_e \approx (1 - Y_4)^{1/2} \frac{0.51}{\eta^{1/2}} \left(\frac{T}{m_e} \right)^{-3/4} e^{-B/2T} , \quad (7)$$

where $B = 13.6$ eV is the hydrogen binding energy and Y_4 is the ^4He abundance. Thus we obtain the familiar result that in our Universe the MRD takes place in the matter domination period, at the temperature $T_{\text{dec}} \simeq 0.26$ eV, which corresponds to redshift $1 + z_{\text{dec}} = T_{\text{dec}}/T_0 \simeq 1100$.

The MRD temperature in the M sector T'_{dec} can be calculated following the same lines as in the ordinary one. Due to the fact that in either case the photon decoupling occurs

⁴In the most general case, where there is also some other dark matter component, as the CDM, the parameter β could be the sum of two terms, $\beta + \beta_{\text{CDM}}$.

when the exponential factor in eq. (7) becomes very small, we have $T'_{\text{dec}} \simeq T_{\text{dec}}$, up to small corrections related to η' , Y'_4 different from η , Y_4 (for more details see ref. [19]). Hence, considering that $T' = x \cdot T$, we obtain

$$1 + z'_{\text{dec}} \simeq x^{-1}(1 + z_{\text{dec}}) \simeq 1.1 \cdot 10^3 x^{-1}, \quad (8)$$

so that *the MRD in the M sector occurs earlier than in the ordinary one*. Moreover, comparing eqs. (4) and (8), which have different dependences on x , we find that, for x smaller than a typical value x_{eq} expressed by

$$x_{\text{eq}} \approx 0.046(\Omega_m h^2)^{-1}, \quad (9)$$

the mirror photons would decouple yet during the radiation dominated period (see fig. 1). Assuming, e.g., the value $\Omega_m h^2 = 0.135$ (the result of a recent WMAP fit [23]), we obtain $x_{\text{eq}} \approx 0.34$, which indicates that below about this value the mirror decoupling happens in the radiation dominated period, with consequences on structure formation (as we will see in the following sections and in paper 2 [22]).

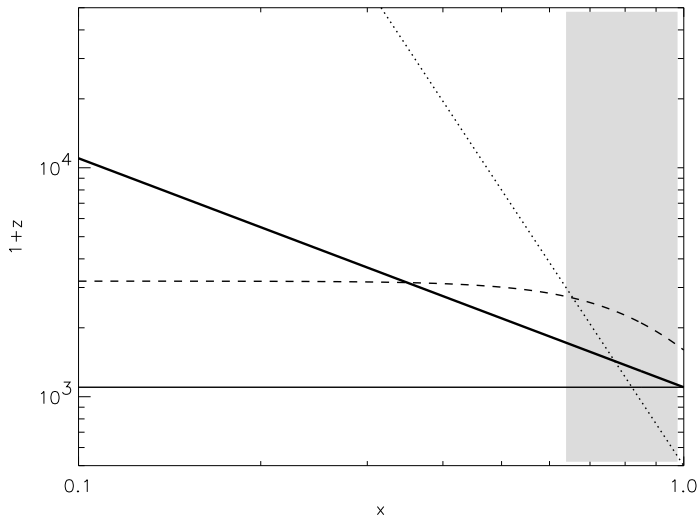


Figure 1: The M photon decoupling redshift $1+z'_{\text{dec}}$ as a function of x (thick solid). The horizontal thin solid line marks the ordinary photon decoupling redshift $1+z_{\text{dec}} = 1100$. We also show the matter-radiation equality redshift $1+z_{\text{eq}}$ (dash) and the mirror Jeans-horizon mass equality redshift $1+z'_c$ (dot) for the case $\Omega_m h^2 = 0.135$. The shaded area $x > 0.64$ is excluded by the BBN limits.

We have shown that mirror baryons could provide a significant contribution to the energy density of the Universe and thus they could constitute a relevant component of dark matter. Immediate question arises: how the mirror baryonic dark matter (MBDM) behaves and what are the differences from the more familiar dark matter candidates as the cold dark matter (CDM), the hot dark matter (HDM), etc. In next sections we discuss the problem of the cosmological structure formation in the presence of M baryons as a dark matter component.

3 Mirror baryonic structure formation

In this section, we extend the linear structure formation theory (for the standard scenario, see refs. [24] and [25]) to the case of dark matter with a non-negligible mirror baryonic component.

In a Mirror Universe we assume that a mirror sector is present, so that the matter is made of ordinary baryons (the only certain component), non-baryonic (dark) matter, and mirror baryons. Thus, it is necessary to study the structure formation in all these three components. We proceed in this way: first of all, we recall the situation for ordinary baryons, and then we compute the same quantities for mirror baryons, comparing them with each other and with the CDM case.

In general, when dealing with the pre-recombination plasma, we distinguish between two types of perturbations, namely between “isoentropic” (*adiabatic*) and “entropic” (*isocurvature* or *isothermal*) modes [26], while after matter-radiation decoupling perturbations evolve in the same way regardless of their original nature.

In this paper we study only adiabatic perturbations, which are today the preferred perturbation modes, and we leave out the isocurvature modes, which could also have a contribution, but certainly cannot be the dominant component [27]. Here we remember only that an adiabatic perturbation satisfies the *condition for adiabaticity*

$$\delta_m = \frac{3}{4}\delta_r, \quad (10)$$

which, defining, as usual, $\delta \equiv (\delta\rho/\rho)$, relates perturbations in matter (δ_m) and radiation (δ_r) components.

We will now consider cosmological models where baryons, ordinary or mirror, are the dominant form of matter. Thus, it is crucial to study the interaction between baryonic matter and radiation during the plasma epoch in both sectors, and the simplest way of doing it is by looking at models containing only these two matter components.

According to the Jeans theory [28], the relevant scale for the gravitational instabilities is characterized by the Jeans scale (length and mass), which now needs to be defined in both the ordinary and mirror sectors. Then, we define the ordinary and mirror Jeans lengths as

$$\lambda_J \simeq v_s \sqrt{\frac{\pi}{G\rho_{\text{dom}}}} \quad \lambda'_J \simeq v'_s \sqrt{\frac{\pi}{G\rho_{\text{dom}}}}, \quad (11)$$

where ρ_{dom} is the density of the dominant species, and v_s, v'_s are the sound speeds, and the Jeans masses as

$$M_J = \frac{4}{3}\pi\rho_b \left(\frac{\lambda_J}{2}\right)^3 = \frac{\pi}{6}\rho_b (\lambda_J)^3 \quad M'_J = \frac{4}{3}\pi\rho'_b \left(\frac{\lambda'_J}{2}\right)^3, \quad (12)$$

where the density is now that of the perturbed component (ordinary or mirror baryons).

3.1 Evolution of the adiabatic sound speed

Looking at the expressions of the Jeans length (11), it is clear that the key issues are the evolutions of the sound speeds in both sectors, since they determine the scales of gravitational instabilities. Using the definition of adiabatic sound speed, we obtain for the two sectors

$$v_s = \left(\frac{\partial p}{\partial \rho}\right)^{1/2} = w^{1/2} \quad v'_s = \left(\frac{\partial p'}{\partial \rho'}\right)^{1/2} = (w')^{1/2}, \quad (13)$$

where w and w' are relative respectively to the ordinary and mirror equations of state $p = w\rho$ and $p' = w'\rho'$.

First of all, we consider the standard case of a Universe made of only one sector. In a mixture of radiation and baryonic matter the total density and pressure are $\rho = \rho_\gamma + \rho_b$

and $p \simeq p_\gamma = \rho_\gamma/3$ respectively (recall that $p_b \simeq 0$). Hence, the adiabatic sound speed is given by

$$v_s = \left(\frac{\partial p}{\partial \rho} \right)^{1/2} \simeq \frac{1}{\sqrt{3}} \left(1 + \frac{3\rho_b}{4\rho_\gamma} \right)^{-1/2}, \quad (14)$$

where we have used the adiabatic condition (10). In particular, using the scaling laws $\rho_m \propto \rho_{0m}(1+z)^3$ and $\rho_\gamma \propto \rho_{0\gamma}(1+z)^4$, together with the definition of matter-radiation equality (where we now consider only baryons and photons), we obtain

$$v_s(z) \simeq \frac{1}{\sqrt{3}} \left[1 + \frac{3}{4} \left(\frac{1+z_{\text{eq}}}{1+z} \right) \right]^{-1/2}. \quad (15)$$

In fact, the relation above is valid only for an ordinary Universe, and it is an approximation, for small values of x and the mirror baryon density (remember that $\beta = \Omega'_b/\Omega_b$), of the more general equation for a Universe made of two sectors of baryons and photons, obtained using eqs. (14) and (5) and given by

$$v_s(z) \simeq \frac{1}{\sqrt{3}} \left[1 + \frac{3}{4} \left(\frac{1+x^4}{1+\beta} \right) \left(\frac{1+z_{\text{eq}}}{1+z} \right) \right]^{-1/2}. \quad (16)$$

In the most general case, the matter is made not only of ordinary and mirror baryons, but also of some other form of dark matter, so the factor $1 + \beta$ is replaced by $1 + \beta + \beta_{DM}$, where $\beta_{DM} = (\Omega_m - \Omega_b - \Omega'_b)/\Omega_b$. The presence of the term $[(1+x^4)/(1+\beta)]$ in equation (16) is linked to the shift of matter-radiation equality epoch (6), thus it only balance this effect, without changing the value of the sound speed computed using eq. (15).

The mirror plasma contains more baryons and less photons than the ordinary one, $\rho'_b = \beta\rho_b$ and $\rho'_\gamma = x^4\rho_\gamma$. Then, using eqs. (13) and (5), we have

$$v'_s(z) \simeq \frac{1}{\sqrt{3}} \left(1 + \frac{3\rho'_b}{4\rho'_\gamma} \right)^{-1/2} \approx \frac{1}{\sqrt{3}} \left[1 + \frac{3}{4} \left(\frac{1+x^{-4}}{1+\beta^{-1}} \right) \left(\frac{1+z_{\text{eq}}}{1+z} \right) \right]^{-1/2}. \quad (17)$$

Let us consider for simplicity the case when dark matter of the Universe is entirely due to M baryons, $\Omega_m \simeq \Omega'_b$ (i.e., $\beta \gg 1$). Hence, for the redshifts of cosmological relevance, $z \sim z_{\text{eq}}$, we have $v'_s \sim 2x^2/3$, which is always less than $v_s \sim 1/\sqrt{3}$ (some example: if $x = 0.7$, $v'_s \approx 0.5 \cdot v_s$; if $x = 0.3$, $v'_s \approx 0.1 \cdot v_s$). In expression (17) it is crucial the presence of the factor $[(1+x^{-4})/(1+\beta^{-1})]$, which is always greater than 1 (given the bounds of eqs. (1) on the parameters), so that $v'_s < v_s$ during all the history of the Universe, and only in the limit of very low scale factors, $a \ll a_{\text{eq}}$, we obtain $v'_s \simeq v_s \simeq 1/\sqrt{3}$. As we will see in the following, this has important consequences on structure formation scales.

Now we define $a_{b\gamma}$ as the scale factor corresponding to the redshift

$$(1 + z_{b\gamma}) = (a_{b\gamma})^{-1} = (\Omega_b/\Omega_\gamma) = 3.9 \cdot 10^4 (\Omega_b h^2). \quad (18)$$

Since $1 + z_{\text{rec}} \simeq 1100$, ordinary baryon-photon equipartition occurs before recombination only if $\Omega_b h^2 > 0.026$ (which seems unlikely, given its current estimates). According to what found in § 2, in the mirror sector the scale of baryon-photon equality $a'_{b\gamma}$ is dependent on x and it transforms as

$$a'_{b\gamma} = \frac{\Omega'_\gamma}{\Omega'_b} \simeq \frac{\Omega_\gamma x^4}{\Omega_b \beta} = a_{b\gamma} \frac{x^4}{\beta} < a_{b\gamma}. \quad (19)$$

If we remember the definition of the quantity $x_{\text{eq}} \approx 0.046(\Omega_m h^2)^{-1}$, we have that for $x > x_{\text{eq}}$ the decoupling occurs after equipartition (as in the ordinary sector for $\Omega_b h^2 > 0.026$), while for $x < x_{\text{eq}}$ it occurs before (as for $\Omega_b h^2 < 0.026$).

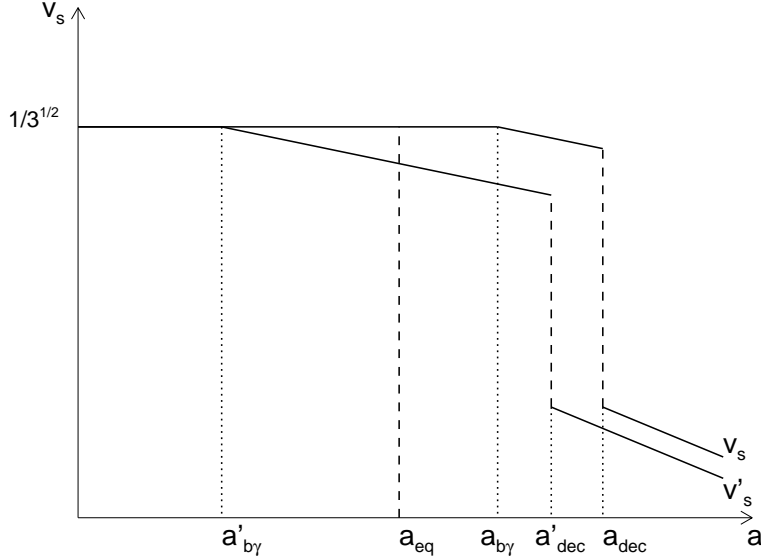


Figure 2: The trends of the mirror sound speed (v'_s) as a function of the scale factor, compared with the ordinary sound speed (v_s). The ordinary model has $\Omega_b h^2 = 0.08$, while the mirror model has $x = 0.6$ and $\beta = 2$. Are also reported all the key epochs: photon-baryon equipartition and decoupling in both sectors, and the matter-radiation equality.

Regardless of which sector we are considering, in the radiation era $\rho_\gamma \gg \rho_b$, ensuring that $v_s \simeq 1/\sqrt{3}$. In the interval between equipartition and decoupling, when $\rho_b \gg \rho_\gamma$, eq. (14) gives $v_s \simeq \sqrt{4\rho_\gamma/3\rho_b} \propto a^{-1/2}$. After decoupling there is no more pressure equilibrium between baryons and photons, and v_s is just the velocity dispersion of a gas of hydrogen and helium, $v_s \propto a^{-1}$. If $\Omega_b h^2 < 0.026$ or $x < x_{\text{eq}}$ (according to what sector we consider), photon-baryon equipartition occurs after decoupling, and the intermediate situation does not arise.

It follows that, by taking care to interchange $a_{b\gamma}$ with $a'_{b\gamma}$ and a_{dec} with a'_{dec} , we have for the sound speed the same trends with the scale factor in both sectors, though with the aforementioned differences in the values. The situation whit $x > x_{\text{eq}}$ is resumed below:

$$v'_s(a) \propto \begin{cases} \text{const.} & a < a'_{b\gamma} , \\ a^{-1/2} & a'_{b\gamma} < a < a'_{\text{dec}} , \\ a^{-1} & a > a'_{\text{dec}} . \end{cases} \quad (20)$$

If we recall that the matter-radiation equality for a single sector (ordinary) Universe, $(a_{\text{eq}})_{\text{ord}}$, is always bigger than that for a two sectors (mirror) one, $(a_{\text{eq}})_{\text{mir}}$, according to

$$(a_{\text{eq}})_{\text{mir}} = \frac{(1+x^4)}{(1+\beta)} (a_{\text{eq}})_{\text{ord}} < (a_{\text{eq}})_{\text{ord}} , \quad (21)$$

together with our hypothesis $x < 1$ (from the BBN bound) and $\beta > 1$ (cosmologically interesting situation, i.e., significant mirror baryonic contribution to the dark matter), we obtain the useful inequality always verified in a Universe made of O and M sectors

$$a'_{b\gamma} < a_{\text{eq}} < a_{b\gamma} . \quad (22)$$

It's very important to remark (see ref. [24]) that at decoupling v_s^2 drops from (p_γ/ρ_b) to (p_b/ρ_b) . Since $p_\gamma \propto n_\gamma T$ while $p_b \propto n_b T$ with $(n_\gamma/n_b) \simeq 10^9 \gg 1$ in the ordinary sector,

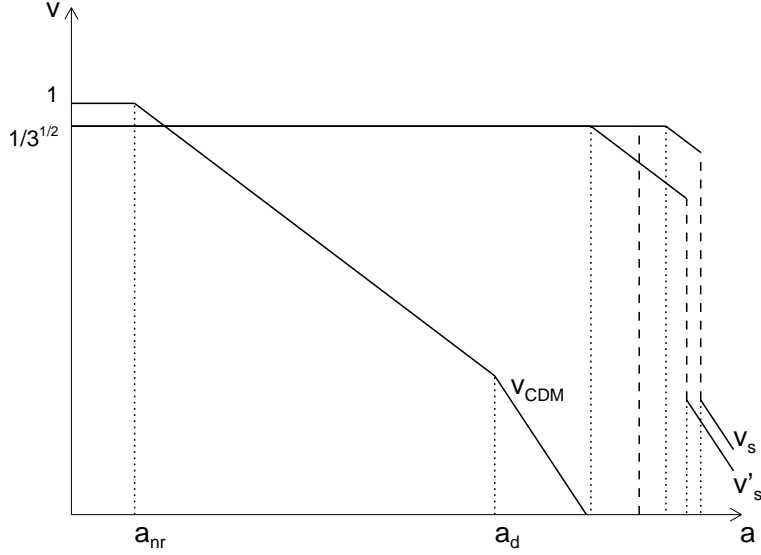


Figure 3: The trends of the mirror (v'_s) and ordinary (v_s) sound speed compared with the velocity dispersion of a typical non baryonic cold dark matter candidate of mass ~ 1 GeV (v_{CDM}); a_{nr} and a_{d} indicate the scale factors at which the dark matter particles become non relativistic or decouple. The ordinary and mirror models are the same as in figure 2, but the horizontal scale is expanded by some decade in order to show the CDM velocity.

this is a large drop in v_s and consequently in λ_J . More precisely, v_s^2 drops from the value $(1/3)(\rho_\gamma/\rho_b) = (1/3)(\Omega_\gamma/\Omega_b)(1 + z_{\text{dec}})$ to the value $(5/3)(T_{\text{dec}}/m_b) = (5/3)(T_0/m_b)(1 + z_{\text{dec}})$, with a reduction factor

$$F_1(\Omega_b h^2 > 0.026) = \frac{(v_s^2)_{\text{dec}}^{(+)}}{(v_s^2)_{\text{dec}}^{(-)}} = 6.63 \cdot 10^{-8}(\Omega_b h^2) , \quad (23)$$

where $(v_s^2)_{\text{dec}}^{(-)}$ and $(v_s^2)_{\text{dec}}^{(+)}$ indicate the sound speed respectively just before and after decoupling. If we consider now the mirror sector and the drop in $(v'_s)^2$ at decoupling, we find for the reduction factor

$$F'_1(x > x_{\text{eq}}) = \beta x^{-3} F_1 . \quad (24)$$

In the case $\Omega_b h^2 < 0.026$, v_s^2 drops directly from $(1/3)$ to $(5/3)(T_{\text{dec}}/m_b) = (5/3)(T_0/m_b)(1 + z_{\text{dec}})$ with a suppression

$$F_2(\Omega_b h^2 < 0.026) = \frac{(v_s^2)_{\text{dec}}^{(+)}}{(v_s^2)_{\text{dec}}^{(-)}} = 1.9 \cdot 10^{-9} . \quad (25)$$

It's easy to find that in the mirror sector the reduction factor in the case $a'_{b\gamma} > a'_{\text{dec}}$ is the same as in the ordinary one

$$F'_2(x < x_{\text{eq}}) = F_2 . \quad (26)$$

Some example: for $x = 0.7$, $F'_1 \approx 2.9\beta F_1$; for $x = 0.5$, $F'_1 = 8\beta F_1$; for $x = 0.3$, $F'_1 \approx 37\beta F_1$. We remark that, if $\beta \geq 1$, F'_1 is at least about an order of magnitude larger than F_1 . In fact, after decoupling $(v'_s)^2 = (5/3)(T'_{\text{dec}}/m_b) = (5/3)(T_{\text{dec}}/m_b) = (v_s)^2$ (since $T'_{\text{dec}} = T_{\text{dec}}$), and between equipartition and recombination $(v'_s)^2 < (v_s)^2$. The relation above means that the drop is smaller in the mirror sector than in the ordinary one. Obviously, before equipartition $(v'_s)^2 = (v_s)^2 = 1/3$, and for this reason the parameter F_2 is the same in both sectors.

In figure 2 we plot the trends with scale factor of the mirror sound speed, in comparison with the ordinary one. The ordinary model is a typical one with $\Omega_b h^2 > 0.026$, while the mirror model has $x = 0.6$ and $\beta = 2$ (this means that M baryonic density is twice the ordinary one, chosen in these models about four times its current estimation in order to better show the general behaviour). In the same figure we show also the aforementioned relative positions of the key epochs (photon-baryon equipartition and decoupling) for both sectors, together with the matter-radiation equality. If we reduce the value $\Omega_b h^2$, $a_{b\gamma}$ goes toward higher values, while a_{dec} remains fixed, so that for $\Omega_b h^2 < 0.026$ decoupling happens before equipartition and the intermediate regime, where $v_s \propto a^{-1/2}$, disappears. In an analogous way, if we reduce x , a'_{dec} shifts to lower values, until for $x < x_{\text{eq}}$ it occurs before the mirror equipartition $a'_{b\gamma}$, so that the intermediate regime for v'_s disappears.

In figure 3 the same ordinary and mirror sound speeds are plotted together with the velocity dispersion of a typical non baryonic cold dark matter candidate of mass $\sim 1\text{GeV}$. Note that the horizontal scale is expanded by some decade compared to the figure 2, because the key epochs for the CDM velocity evolution (the epochs when the particles become non relativistic, a_{nr} , and when they decouple, a_{d}) occur at much lower scale factors.

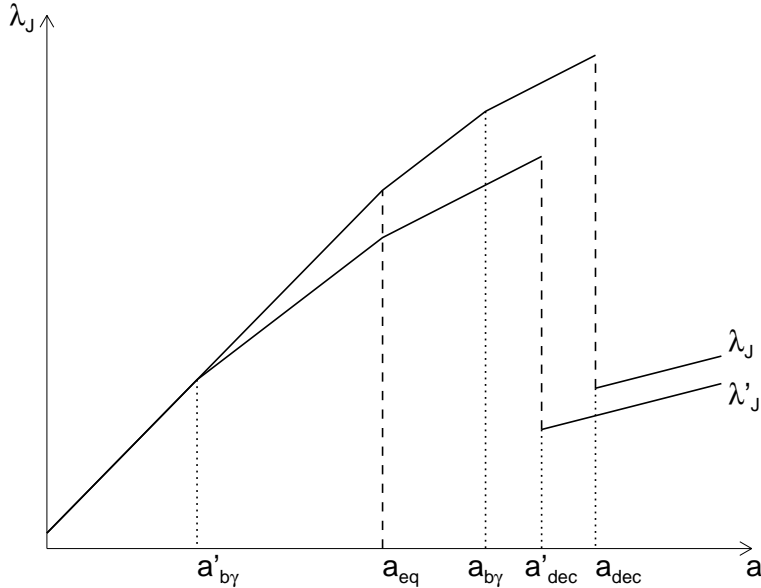


Figure 4: The trends of the mirror Jeans length (λ'_J) as a function of the scale factor, compared with the ordinary Jeans length (λ_J). The ordinary model has $\Omega_b h^2 = 0.08$, while the mirror model has $x = 0.6$ and $\beta = 2$. The horizontal scale is the same as in figure 2. We remark that the same behaviours of the ordinary sector are present in the mirror sector for different intervals of scale factor.

3.2 Evolution of the Jeans length and the Jeans mass

Recalling the definitions (11) and (12), and using the results of § 3.1 relative to the sound speed, we can compute the evolution of the mirror Jeans length and mass and compare them with the analogous quantities for ordinary baryons and CDM.

We find for the evolution of the adiabatic Jeans length and mass of ordinary baryons

in the case $\Omega_b h^2 > 0.026$

$$\lambda_J \propto \begin{cases} a^2 \\ a^{3/2} \\ a \\ a^{1/2} \end{cases} \quad M_J \propto \frac{\lambda_J^3}{a^3} \propto \begin{cases} a^3 \\ a^{3/2} \\ const. \\ a^{-3/2} \end{cases} \quad \begin{cases} a < a_{\text{eq}} \\ a_{\text{eq}} < a < a_{\text{b}\gamma} \\ a_{\text{b}\gamma} < a < a_{\text{dec}} \\ a_{\text{dec}} < a \end{cases} \quad (27)$$

Otherwise, if $\Omega_b h^2 \leq 0.026$, $a_{\text{b}\gamma} > a_{\text{dec}}$, there is no intermediate phase $a_{\text{b}\gamma} < a < a_{\text{dec}}$.

In the mirror sector it's no more sufficient to interchange $a_{\text{b}\gamma}$ with $a'_{\text{b}\gamma}$ and a_{dec} with a'_{dec} , as made for the sound speed, because from relation (22) we know that in the mirror sector the photon-baryon equipartition happens before the matter-radiation equality (due to the fact that we are considering a mirror sector with more baryons and less photons than the ordinary one). It follows that, due to the shifts of the key epochs, the intervals of scale factor for the various trends are different. As usual, there are two different possibilities, $x > x_{\text{eq}}$ and $x < x_{\text{eq}}$ (which correspond roughly to $\Omega_b h^2 > 0.026$ and $\Omega_b h^2 < 0.026$ in an ordinary Universe), where, as discussed in § 3.1, for the second one the intermediate situation is absent.

Using the results of § 3.1 for the sound speed, we find the evolution of the adiabatic Jeans length and mass in the case $x > x_{\text{eq}}$

$$\lambda'_J \propto \begin{cases} a^2 \\ a^{3/2} \\ a \\ a^{1/2} \end{cases} \quad M'_J \propto \frac{(\lambda'_J)^3}{a^3} \propto \begin{cases} a^3 \\ a^{3/2} \\ const. \\ a^{-3/2} \end{cases} \quad \begin{cases} a < a'_{\text{b}\gamma} \\ a'_{\text{b}\gamma} < a < a_{\text{eq}} \\ a_{\text{eq}} < a < a'_{\text{dec}} \\ a'_{\text{dec}} < a \end{cases} \quad (28)$$

We plot in figures 4 and 5 with the same horizontal scale the trends of the mirror Jeans length and mass compared with those for the ordinary sector; the parameters of both mirror and ordinary models are the ones previously used, i.e. $\Omega_b h^2 = 0.08$, $x = 0.6 > x_{\text{eq}}$ and $\beta = 2$.

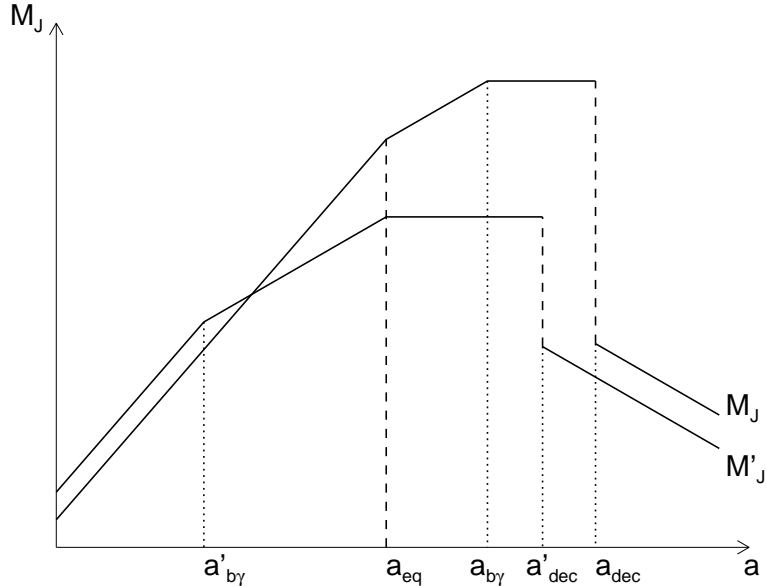


Figure 5: The trends of the mirror Jeans mass (M'_J) as a function of the scale factor, compared with the ordinary Jeans mass (M_J). The models and the horizontal scale are the same as in figure 4.

In the ordinary sector the greatest value of the Jeans mass is just before decoupling (see ref. [24]), in the interval $a_{b\gamma} < a < a_{\text{dec}}$, where

$$M_{\text{J}}(a \lesssim a_{\text{dec}}) = 1.47 \cdot 10^{14} M_{\odot} (1 + \beta)^{-3/2} (\Omega_{\text{b}} h^2)^{-2}, \quad (29)$$

that for an hypothetical $\Omega_{\text{b}} \simeq 0.1 h^{-2}$ and $\beta = 0$ is $\sim 10^{16} M_{\odot}$. Just after decoupling we have

$$M_{\text{J}}(a \gtrsim a_{\text{dec}}) = 2.5 \cdot 10^3 M_{\odot} (1 + \beta)^{-3/2} (\Omega_{\text{b}} h^2)^{-1/2}, \quad (30)$$

that for $\Omega_{\text{b}} \simeq 0.1 h^{-2}$ and $\beta = 0$ is $\sim 10^4 M_{\odot}$. This drop is very sudden and large, changing the Jeans mass by $F_1^{3/2} \simeq 1.7 \cdot 10^{-11} (\Omega_{\text{b}} h^2)^{3/2}$.

Otherwise, if $\Omega_{\text{b}} h^2 \leq 0.026$, $a_{b\gamma} > a_{\text{dec}}$, there is no intermediate phase $a_{b\gamma} < a < a_{\text{dec}}$, and $M_{\text{J}}(a \lesssim a_{\text{dec}})$ is larger

$$M_{\text{J}}(a \lesssim a_{\text{dec}}) \simeq 3.1 \cdot 10^{16} M_{\odot} (1 + \beta)^{-3/2} (\Omega_{\text{b}} h^2)^{-1/2}, \quad (31)$$

while after decoupling it takes the value in eq. (30), so that the drop is larger, $F_2^{3/2} \simeq 8.3 \cdot 10^{-14}$. We observe that, with the assumptions $\Omega_{\text{b}} = 1$ (totally excluded by observations) and $\beta = 0$, $M_{\text{J,max}}$ (which is the first scale to become gravitationally unstable and collapse soon after decoupling) has the size of a supercluster of galaxies.

If we now consider the expression (19), we have

$$\frac{a'_{b\gamma}}{a_{\text{eq}}} = \left(\frac{1 + \beta}{\beta} \right) \left(\frac{x^4}{1 + x^4} \right), \quad (32)$$

which can be used to express the value of the mirror Jeans mass in the interval $a_{\text{eq}} < a < a'_{\text{dec}}$ (where M'_{J} takes the maximum value) in terms of the ordinary Jeans mass in the corresponding ordinary interval $a_{b\gamma} < a < a_{\text{dec}}$. We obtain

$$M'_{\text{J}}(a \lesssim a'_{\text{dec}}) \approx \beta^{-1/2} \left(\frac{x^4}{1 + x^4} \right)^{3/2} \cdot M_{\text{J}}(a \lesssim a_{\text{dec}}), \quad (33)$$

which, for $\beta \geq 1$ and $x < 1$, means that the Jeans mass for the M baryons is lower than for the O ones over the entire permitted (β - x) parameter space, with implications for the structure formation process. If, e.g., $x = 0.6$ and $\beta = 2$, then $M'_{\text{J}} \sim 0.03 M_{\text{J}}$. We can also express the same quantity in terms of Ω_{b} , x and β , in the case that all the dark matter is in the form of mirror baryons, as

$$M'_{\text{J}}(a \lesssim a'_{\text{dec}}) \approx 3.2 \cdot 10^{14} M_{\odot} \beta^{-1/2} (1 + \beta)^{-3/2} \left(\frac{x^4}{1 + x^4} \right)^{3/2} (\Omega_{\text{b}} h^2)^{-2}. \quad (34)$$

If we remember eq. (24), we obtain that for the mirror model the drop in the Jeans mass at decoupling is $(F'_1)^{3/2} = \beta^{3/2} x^{-9/2} (F_1)^{3/2}$, which, given our bounds on x and β , is greater than $(F_1)^{3/2}$. We give here some numerical example: for $x = 0.7$, $(F'_1)^{3/2} \approx 5\beta^{3/2} (F_1)^{3/2}$; for $x = 0.6$ and $\beta = 2$ (the case of figures 4 and 5), $(F'_1)^{3/2} \approx 28(F_1)^{3/2}$.

It's important to stress that these quantities are strongly dependent on the values of the free parameters x and β , which shift the key epochs and change their relative positions. We can describe some case useful to understand the general behaviour, but if we want an accurate solution of a particular model, we must unambiguously identify the different regimes and solve in detail the appropriate equations.

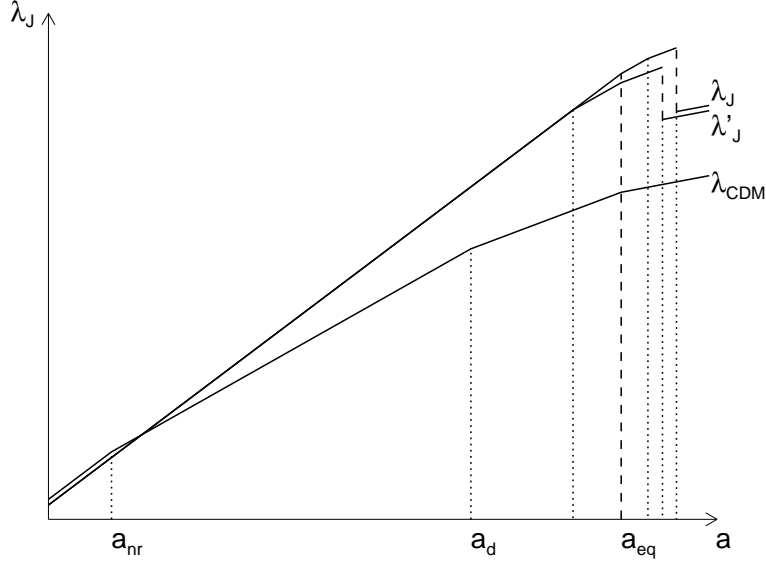


Figure 6: The trends of the mirror (λ'_J) and ordinary (λ_J) Jeans length compared with that of a typical non baryonic cold dark matter candidate of mass ~ 1 GeV (λ'_{CDM}); a_{nr} and a_{d} indicate the scale factors at which the dark matter particles become non relativistic or decouple, respectively. The models are the same as in figure 4, but the horizontal scale is expanded by some decade to show the CDM Jeans length, as in figure 3.

In figures 6 and 7 we plot the trends of the mirror and ordinary Jeans length and mass compared with those of a typical non baryonic cold dark matter candidate of mass ~ 1 GeV. Apart from the usual expansion of the horizontal scale, due to the much lower values of the CDM key epochs as compared to the baryonic ones, a comparison of the mirror scenario with the cold dark matter one shows that the maximal value of the CDM Jeans mass is several orders of magnitude lower than that for mirror baryons. This implies that a very large range of mass scales, which in a mirror baryonic scenario oscillate before decoupling, in a cold dark matter scenario would grow unperturbed during all the time (for more details see § 5).

For the case $x < x_{\text{eq}}$, both $a'_{\text{b}\gamma}$ and a'_{dec} are smaller than the previous case $x > x_{\text{eq}}$, while the matter-radiation equality remains practically the same; as explained in § 2, the mirror decoupling (with the related drop in the associated quantities) happens before the matter-radiation equality, and the trends of the mirror Jeans length and mass are the following

$$\lambda'_J \propto \begin{cases} a^2 \\ a^{3/2} \\ a \\ a^{1/2} \end{cases} \quad M'_J \propto \frac{(\lambda'_J)^3}{a^3} \propto \begin{cases} a^3 & a < a'_{\text{b}\gamma} \\ a^{3/2} & a'_{\text{b}\gamma} < a < a'_{\text{dec}} \\ \text{const.} & a'_{\text{dec}} < a < a_{\text{eq}} \\ a^{-3/2} & a_{\text{eq}} < a \end{cases} \quad (35)$$

In this case we obtain for the highest value of the Jeans mass just before decoupling the expression

$$M'_J(a \lesssim a'_{\text{dec}}) \approx 3.2 \cdot 10^{14} M_{\odot} \beta^{-1/2} (1 + \beta)^{-3/2} \left(\frac{x}{x_{\text{eq}}} \right)^{3/2} \left(\frac{x^4}{1 + x^4} \right)^{3/2} (\Omega_{\text{b}} h^2)^{-2}. \quad (36)$$

In case $x = x_{\text{eq}}$, the expressions (34) and (36), respectively valid for $x \geq x_{\text{eq}}$ and $x \leq x_{\text{eq}}$, are coincident, as we expect. If we consider the differences between the highest mirror

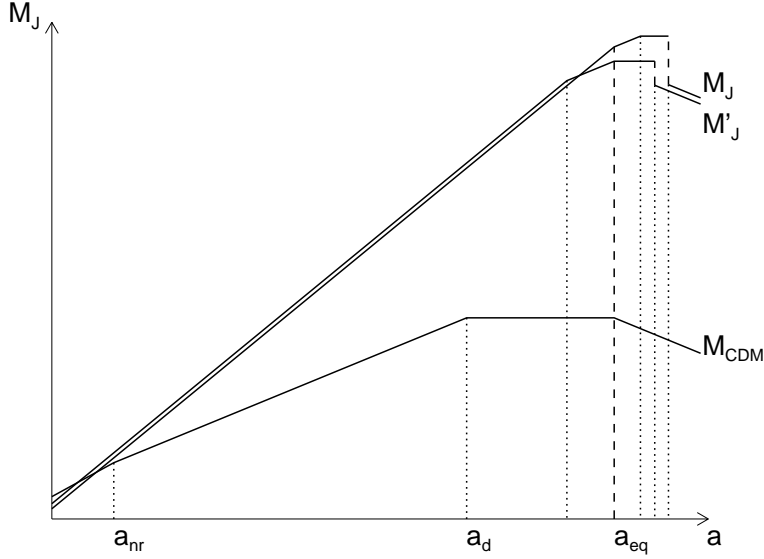


Figure 7: The trends of the mirror (M'_J) and ordinary (M_J) Jeans mass compared with those of a typical non baryonic cold dark matter candidate of mass ~ 1 GeV (M_{CDM}); a_{nr} and a_d indicate the scale factors at which the dark matter particles become non relativistic or decouple, respectively. The model parameters and the horizontal scale are the same as in figure 6.

Jeans mass for the particular values $x = x_{\text{eq}}/2$, $x = x_{\text{eq}}$ and $x = 2x_{\text{eq}}$, we obtain the following relations:

$$M'_{J,\text{max}}(x_{\text{eq}}/2) \approx \left(\frac{1}{2}\right)^{15/2} \left(\frac{1 + x_{\text{eq}}^4}{1 + (x_{\text{eq}}/2)^4}\right)^{3/2} M'_{J,\text{max}}(x_{\text{eq}}) \approx 0.005 M'_{J,\text{max}}(x_{\text{eq}}), \quad (37)$$

$$M'_{J,\text{max}}(2x_{\text{eq}}) \approx 2^6 \left(\frac{1 + x_{\text{eq}}^4}{1 + (2x_{\text{eq}})^4}\right)^{3/2} M'_{J,\text{max}}(x_{\text{eq}}) \approx 64 M'_{J,\text{max}}(x_{\text{eq}}). \quad (38)$$

In figure 8 we plot the mirror Jeans mass for the three different possibilities: $x < x_{\text{eq}}$, $x > x_{\text{eq}}$ and $x = x_{\text{eq}}$ (the transition between the two regimes), keeping constant all other parameters. In these three models the matter-radiation equality is the only key epoch which remains almost constant. The change in the trends when x becomes lower than x_{eq} , due to the fact that a'_{dec} becomes lower than a_{eq} , generates an evident decrease of the Jeans mass.

3.3 Evolution of the Hubble mass

The trends of the Hubble length and mass are expressed, as usually, by

$$\lambda_{\text{H}} \propto \begin{cases} a^2 & a < a_{\text{eq}} \\ a^{3/2} & a > a_{\text{eq}} \end{cases} \quad M_{\text{H}} \propto \frac{(\lambda_{\text{H}})^3}{a^3} \propto \begin{cases} a^3 & a < a_{\text{eq}} \\ a^{3/2} & a > a_{\text{eq}} \end{cases} \quad (39)$$

It should be emphasized that, as for the ordinary baryons, during the period of domination of photons ($a < a'_{\text{b}\gamma}$) the mirror baryonic Jeans mass is of the same order of the Hubble mass. In fact, following definitions we find

$$\frac{M'_J}{M_{\text{H}}} = \frac{(\lambda'_J)^3}{\lambda_{\text{H}}^3} \simeq 26. \quad (40)$$

We plot the trends of the Hubble mass in figures 10 and 11 together with other fundamental mass scales.

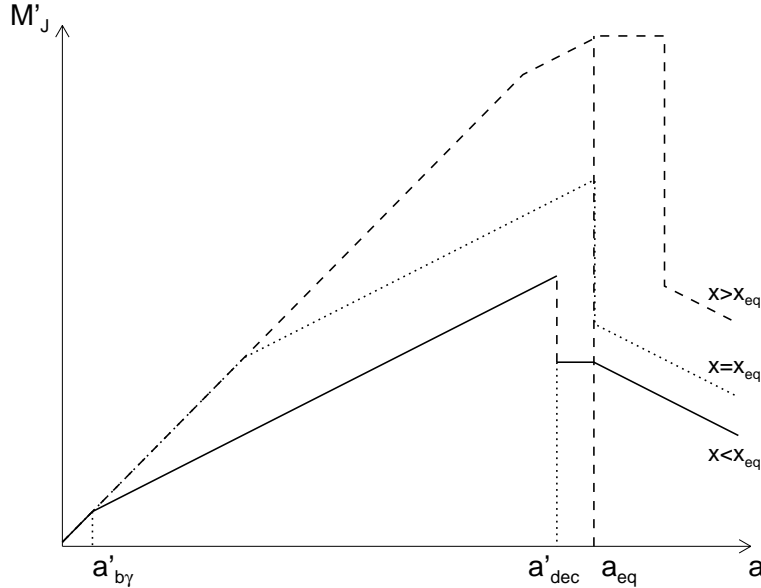


Figure 8: The trends of the mirror Jeans mass for the cases $x < x_{\text{eq}}$ (solid line), $x = x_{\text{eq}}$ (dotted) and $x > x_{\text{eq}}$ (dashed). The model with $x > x_{\text{eq}}$ is the same as in figure 5, the others are obtained changing only the value of x and keeping constant all the other parameters. As clearly shown in the figure, the only key epoch which remains almost constant in the three models is the matter-radiation equality; the mirror baryon-photon equipartition and decoupling indicated are relative to the model with $x < x_{\text{eq}}$. It's also evident the change in the trends when x becomes lower than x_{eq} , due to the fact that a'_{dec} becomes lower than a_{eq} .

3.4 Dissipative effects: collisional damping

A peculiar feature of the mirror baryonic scenario is that mirror baryons undergo the collisional damping as ordinary ones. This dissipative process modify the purely gravitational evolution of perturbations. The physical phenomenon is the interaction between baryons and photons before the recombination, and the consequent dissipation due to viscosity and heat conduction. Around the time of recombination the perfect fluid approximation breaks down, and the perturbations in the photon-baryon plasma suffer from collisional damping. As decoupling is approached, the photon mean free path increases and photons can diffuse from the overdense into the underdense regions, thereby smoothing out any inhomogeneities in the photon-baryon plasma. This effect is known as Silk damping [29].

In order to obtain an estimate of the effect, we follow ref. [30] for ordinary baryons, and then we extend to mirror baryons. We consider the photon mean free path

$$\lambda_\gamma = \frac{1}{X_e n_e \sigma_T} \simeq 10^{29} a^3 X_e^{-1} (\Omega_b h^2)^{-1} \text{ cm} , \quad (41)$$

where X_e is the electron ionization factor, $n_e \propto a^{-3}$ is the number density of the free electrons and σ_T is the cross section for Thomson scattering. Clearly, photon free streaming should completely damp all baryonic perturbations with wavelengths smaller than λ_γ . Damping, however, occurs on scales much larger than λ_γ since the photons slowly diffuse from the overdense into the underdense regions, dragging along the still tightly coupled baryons. Integrating up to decoupling time we obtain the total distance traveled by a typical photon

$$\lambda_S = \sqrt{\frac{3}{5} \frac{(\lambda_\gamma)_{\text{dec}} t_{\text{dec}}}{a_{\text{dec}}^2}} \simeq 3.5 (\Omega_b h^2)^{-3/4} \text{ Mpc} , \quad (42)$$

and the associated mass scale, the Silk mass, given by

$$M_S = \frac{4}{3}\pi\rho_b \left(\frac{\lambda_S}{2}\right)^3 \simeq 6.2 \times 10^{12} (\Omega_b h^2)^{-5/4} M_\odot, \quad (43)$$

which, assuming $\Omega_b h^2 \simeq 0.02$, gives $M_S \simeq 8 \times 10^{14} M_\odot$. This dissipative process causes that fluctuations on scales below the Silk mass are completely washed out at the time of recombination and no structure can form on these scales. This has consequences on large scale structure power spectrum, where small scales have very little power.

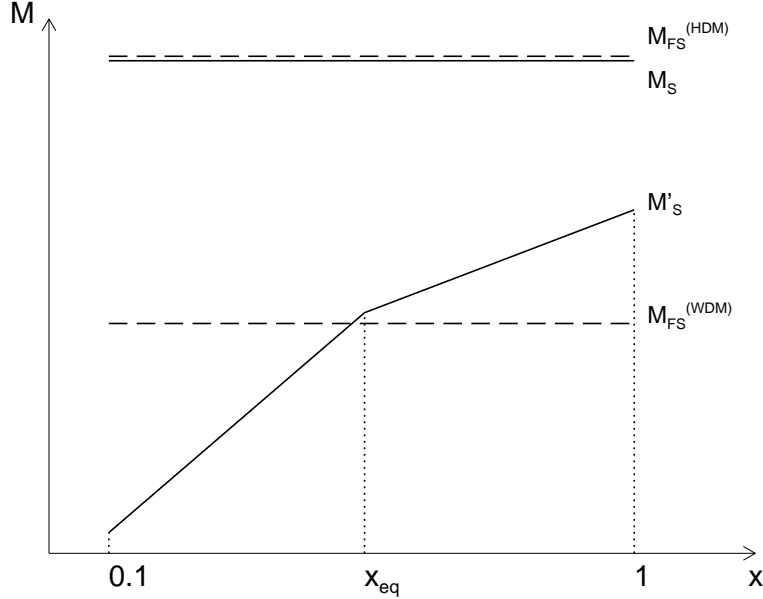


Figure 9: The trend of the mirror Silk mass (M'_S) over a cosmologically interesting range of x , which contains x_{eq} (we considered $\Omega_m h^2 \simeq 0.15$, so $x_{eq} \simeq 0.3$). The axis are both logarithmic. We show for comparison also the values of the ordinary Silk mass (M_S) and of the free streaming mass (M_{FS}) for typical HDM and WDM candidates.

In the mirror sector too, obviously, the photon diffusion from the overdense to underdense regions induces a dragging of charged particles and washes out the perturbations at scales smaller than the mirror Silk scale

$$\lambda'_S \simeq 3f(x)(\beta\Omega_b h^2)^{-3/4} \text{ Mpc}, \quad (44)$$

where $f(x) = x^{5/4}$ for $x > x_{eq}$ and $f(x) = (x/x_{eq})^{3/2}x_{eq}^{5/4}$ for $x < x_{eq}$. Thus, the density perturbation scales running the linear growth after the matter-radiation equality epoch are limited by the length λ'_S . The smallest perturbations that survive the Silk damping will have the mass

$$M'_S \sim [f(x)/2]^3(\beta\Omega_b h^2)^{-5/4}10^{12} M_\odot, \quad (45)$$

which should be less than $2 \times 10^{12} M_\odot$ in view of the BBN bound $x < 0.64$. Interestingly, for $x \sim x_{eq}$ we obtain, for the current estimate of $\Omega_m h^2$ and if all the dark matter is made of mirror baryons, $M'_S \sim 10^{10} M_\odot$, a typical galaxy mass.

At this point it is very interesting a comparison between different damping scales, collisional (ordinary and mirror baryons) and collisionless (non-baryonic dark matter). We know that for hot dark matter (as a neutrino with mass ~ 10 eV) $M_{FS}^\nu \sim 10^{15} M_\odot$, while for a typical warm dark matter candidate with mass ~ 1 keV, $M_{FS}^{WDM} \sim 10^9 - 10^{10} M_\odot$.

From eq. (45) it is evident that the dissipative scale for mirror Silk damping is analogous to that for WDM free streaming. Consequently, the cutoff effects on the corresponding large scale structure power spectra are similar, though with important differences due to the presence of oscillatory features, which makes them distinguishable one from the other (for a detailed presentation of these power spectra see the Paper 2 [22]). In figure 9 we show this comparison together with the trend of the mirror Silk mass over a cosmologically interesting range of x .

4 Scenarios

After the description of the fundamental scales for structure formation, let us now collect all the informations and discuss the mirror scenarios. They are essentially two, according to the value of x , which can be higher or lower than x_{eq} , and are shown respectively in figures 10 and 11, which will be our references during the present section.

Typically, adiabatic perturbations for mirror baryons with sizes larger than the maximum value of the Jeans mass, which is $M'_J(a_{\text{eq}})$ for $x > x_{\text{eq}}$ and $M'_J(a'_{\text{dec}})$ for $x < x_{\text{eq}}$, experience uninterrupted growth. In particular, they grow as $\delta_b \propto a^2$ before matter-radiation equality and as $\delta_b \propto a$ after equality. Fluctuations on scales in the mass interval $M'_S < M < M_{J,\text{max}}$ grow as $\delta_b \propto a^2$ while they are still outside the Hubble radius. After entering the horizon and until recombination these modes oscillate like acoustic waves. The amplitude of the oscillation is constant before equilibrium but decreases as $a^{-1/4}$ between equipartition and recombination. After decoupling the modes become unstable again and grow as $\delta_b \propto a$. Finally all perturbations on scales smaller than the value of the Silk mass are dissipated by photon diffusion.

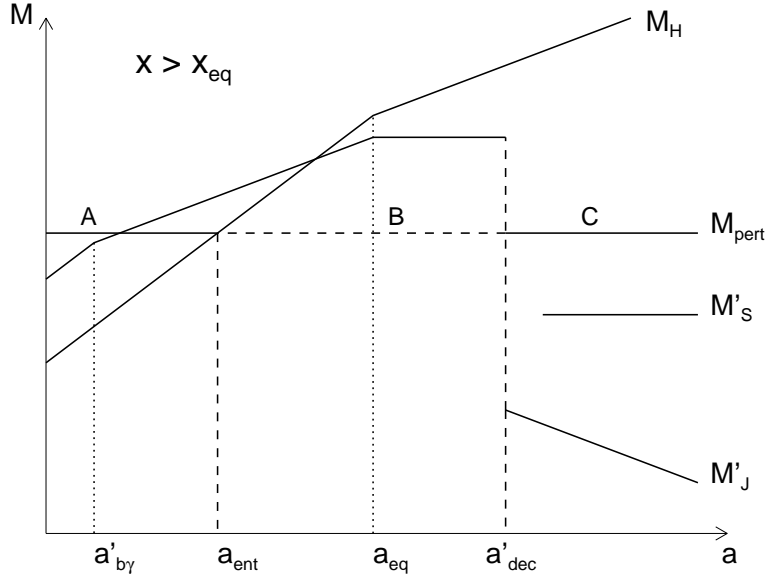


Figure 10: Typical evolution of a perturbed scale M_{pert} in adiabatic mirror baryonic dark matter scenario with $x > x_{\text{eq}}$. The figure shows the Jeans mass M'_J , the Silk mass M'_S and the Hubble mass M_H . The time of horizon crossing of the perturbation is indicated by a_{ent} . Are also indicated the three evolutionary stages: during stage A ($a < a_{\text{ent}} < a_{\text{eq}}$) the mode grows as $\delta_b \propto a^2$; throughout stage B ($a_{\text{ent}} < a < a'_{\text{dec}}$) the perturbation oscillates; finally, in stage C ($a > a'_{\text{dec}}$) the mode becomes unstable again and grows as $\delta_b \propto a$. Fluctuations with size smaller than M'_S are wiped out by photon diffusion.

Given this general behaviour, the schematic evolution of an adiabatic mode with a reference mass scale M_{pert} , with $M'_S < M_{\text{pert}} < M'_J(a_{\text{eq}})$, is depicted in figure 10 for $x > x_{\text{eq}}$. We distinguish between three evolutionary stages, called A, B and C, depending on the size of the perturbation and on the cosmological parameters $\Omega_b h^2$, x and β , which determine the behaviour of the mass scales, and in particular the key moments (time of horizon crossing and decoupling) and the dissipative Silk scale. During stage A, i.e. before the horizon crossing ($a < a_{\text{ent}} < a_{\text{eq}}$), the mode grows as $\delta_b \propto a^2$; throughout stage B ($a_{\text{ent}} < a < a'_{\text{dec}}$) the perturbation enters the horizon, baryons and photons feel each other, and it oscillates; finally, in stage C ($a > a'_{\text{dec}}$), the photons and baryons decouple, and the mode becomes unstable again growing as $\delta_b \propto a$. We remark that fluctuations with sizes greater than $M'_J(a_{\text{eq}})$ grow uninterruptedly (because after horizon crossing the photon pressure cannot balance the gravity), changing the trend from a^2 before MRE to a after it, while those with sizes smaller than M'_S are completely washed out by photon diffusion.

After decoupling, all surviving perturbations (those with $M_{\text{pert}} > M'_S$) grow steadily until their amplitude becomes so large that the linear theory breaks down and one needs to employ a different type of analysis.

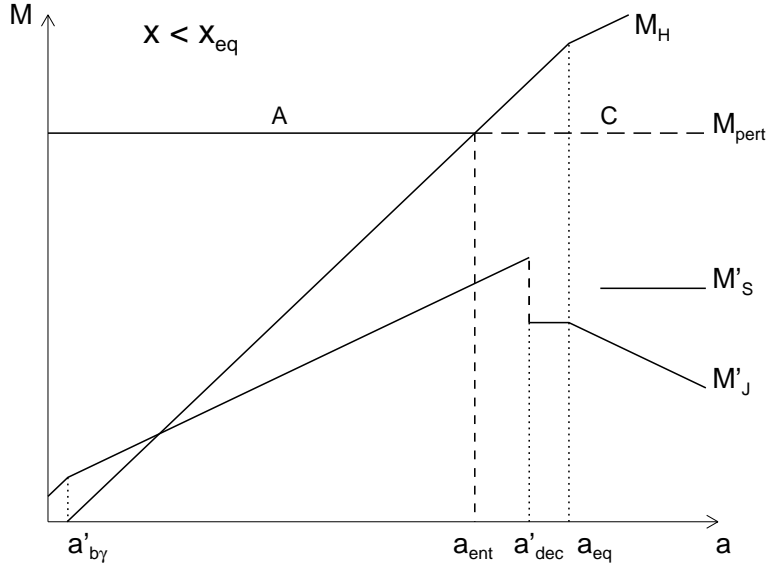


Figure 11: Typical evolution of a perturbed scale M_{pert} in adiabatic mirror baryonic dark matter scenario with $x < x_{\text{eq}}$. The value of M_{pert} is the same as in figure 10. The time of horizon crossing of the perturbation is indicated by a_{ent} . The figure shows the Jeans mass M'_J , the Silk mass M'_S and the Hubble mass M_H . Unlike the case $x > x_{\text{eq}}$ (shown in the previous figure), now there are only the two evolutionary stages A ($a < a_{\text{ent}}$) and C ($a > a_{\text{ent}}$). Fluctuations with size smaller than M'_S are wiped out by photon diffusion, but in this case the Silk mass is near to the maximum Jeans mass.

If we look, instead, at the schematic evolution of an adiabatic mode with the same reference mass scale M_{pert} but for $x < x_{\text{eq}}$, as reported in figure 11, we immediately notice the lower values of the maximum Jeans mass and the Silk mass, which are similar. Therefore, for the plotted perturbative scale there are now only the two stages A and C. In general, depending on its size, the perturbation mass can be higher or lower than the Silk mass (and approximately also than the maximum Jeans mass), so modes with $M_{\text{pert}} > M'_S$ grow continuously before and after their horizon entry, while modes with $M_{\text{pert}} < M'_S$ are completely washed out.

We find that M'_J becomes smaller than the Hubble horizon mass M_H starting from a redshift

$$z_c = 3750 x^{-4} (\Omega_m h^2), \quad (46)$$

which is about z_{eq} for $x = 0.64$, but it sharply increases for smaller values of x , as shown in figure 1. We can recognize this behaviour also watching at the intersections of the lines for M'_J and M_H in figures 10 and 11. Thus, density perturbation scales which enter horizon at $z \sim z_{\text{eq}}$ have masses larger than M'_J and thus undergo uninterrupted linear growth immediately after t_{eq} . Smaller scales for which $M'_J > M_H$ would instead first oscillate. Therefore, the large scale structure formation is not delayed even if the mirror decoupling did not occur yet, i.e. even if $x > x_{\text{eq}}$.

When compared with non baryonic dark matter scenarios, the main feature of the mirror baryonic scenario is that the M baryon density fluctuations should undergo the strong collisional damping around the time of M recombination, which washes out the perturbations at scales smaller than the mirror Silk scale. It follows that density perturbation scales which undergo the linear growth after the MRE epoch are limited by the length λ'_S . This could help in avoiding the excess of small scales (of few Mpc) in the CDM power spectrum without tilting the spectral index. To some extent, the cutoff effect is analogous to the free streaming damping in the case of warm dark matter (WDM), but there are important differences. The point is that, alike usual baryons, the MBDM shows acoustic oscillations with an impact on the large scale structure (LSS) power spectrum [4, 22]. In particular, it is tempting to imagine that the M baryon oscillation effects are related to the anomalous features observed in LSS power spectra.

In addition, the MBDM oscillations transmitted via gravity to the ordinary baryons, could cause observable anomalies in the CMB angular power spectrum for l 's larger than 200. This effect can be observed only if the M baryon Jeans scale λ'_J is larger than the Silk scale of ordinary baryons, which sets a principal cutoff for CMB oscillations around $l \sim 1200$. This would require enough large values of x , near the upper bound fixed by the BBN constraints, and, together with the possible effects on the large scale power spectrum, it can provide a direct test for the MBDM (verifiable by the higher sensitivity of next CMB and LSS observations). For a complete discussion of the CMB and LSS power spectra for a Mirror Universe see the Paper 2 [22].

Clearly, for small x the M matter recombines before the MRE moment, and thus it behaves as the CDM as far as the large scale structure is concerned. However, there still can be crucial differences at smaller scales which already went non-linear, like galaxies. In our scenario, dark matter in galaxies and clusters can contain both CDM and MBDM components, or can be even constituted entirely by the mirror baryons.

One can question whether the MBDM distribution in halos can be different from that of the CDM. Simulations show that the CDM forms triaxial halos with a density profile too clumped toward the center, and overproduces the small substructures within the halo. Since MBDM constitutes a kind of collisional dark matter, it may potentially avoid these problems, at least the one related with the excess of small substructures.

It's also worth noting that, throughout the above discussion, we have assumed that the matter density of the Universe is close to unity. If, instead, the matter density is small and a vacuum density contribution is present, there is an additional complication due to the fact that the Universe may become curvature dominated starting from some redshift z_{curv} . Given the current estimate $\Omega_\Lambda \simeq 0.7$, this transition has yet occurred and the growth of perturbations has stopped around z_{curv} , when the expansion became too rapid for it.

5 Evolution of perturbations

As a result of the studies done in previous sections, in this section we finally consider the temporal evolution of perturbations, as function of the scale factor a . All the plots are the results of numerical computations obtained using a Fortran code originally written for the ordinary Universe and modified to account for the mirror sector.

We used the synchronous gauge and the evolutionary equations presented in ref. [31]. The difference in the use of other gauges is limited to the gauge-dependent behaviour of the density fluctuations on scales larger than the horizon. The fluctuations can appear as growing modes in one coordinate system and as constant mode in another, that is exactly what occurs in the synchronous and the conformal Newtonian gauges.

In the figures we plot the evolution of the components of a Mirror Universe, namely the cold dark matter⁵, the ordinary baryons and photons, and the mirror baryons and photons, changing some parameter to evaluate their influence.

First of all, we comment figure 12b, which is the most useful to recognize the general features of the evolution of perturbations. Starting from the smallest scale factor, we see that all three matter components and the two radiative components grow with the same trend (as a^2), but the radiative ones have a slightly higher density contrast (with a constant rate until they are tightly coupled); this is simply the consequence of considering adiabatic perturbations, which are linked in their matter and radiation components by the adiabatic condition (10). This is the situation when the perturbation is out of horizon, but, when it crosses the horizon, around $a \sim 10^{-4}$, things drastically change. Baryons and photons, in each sector separately, become causally connected, feel each other, and begin to oscillate for the competitive effects of gravity and pressure. Meanwhile, the CDM density perturbation continues to grow uninterruptedly, at first reducing his rate from a^2 to $\ln a$ (due to the rapid expansion during the radiation era), and later, as soon as MRE occurs (at $a \sim 3 \times 10^{-3}$ for the considered model), increasing proportionally to a . The oscillations of baryons and photons continue until their decoupling, which in the mirror sector occurs before than in the ordinary one (scaled by the factor x). This moment is marked in the plot as the point where the lines for the two components move away one from the other. From this point, the photons in both sectors continue the oscillations until they are completely damped, while the M and O baryons rapidly fall into the potential wells created by the cold dark matter and start growing as a . We remark that it's important the way in which the oscillation reaches the decoupling; if it is compressing, first it slows down (as if it continues to oscillate, but disconnected from the photons), and then it expands driven by the gravity; if, otherwise, it is expanding, it directly continues the expansion and we see in the plot that it immediately stops to oscillate. In this figure we have the first behaviour in the mirror sector, the second one in the ordinary sector.

In figures 12, 13 and 14 we compare the behaviours of different scales for the same model. The scales are given by $\log k(\text{Mpc}^{-1}) = -0.5, -1.0, -1.5, -2.0, -2.5, -3.0$, where $k = 2\pi/\lambda$ is the wave number. The effect of early entering the horizon of small scales (those with higher k) is evident. Going toward bigger scales the superhorizon growth continue for a longer time, delaying more and more the beginning of acoustic oscillations, until it occurs out of the coordinate box for the bigger plotted scale ($\log k = -3.0$). Starting from the scale $\log k = -1.5$, the mirror decoupling occurs before the horizon entry of the perturbations, and the evolution of the mirror baryons density is similar to that of the CDM. The same happens to the ordinary baryons too, but for $\log k \lesssim -2.0$ (since they decouple later), while the evolution of mirror baryons is yet indistinguishable from

⁵As non baryonic dark matter we consider only the cold dark matter, which is at present the standard choice in cosmology.

that of the CDM. For the bigger scales ($\log k \lesssim -2.5$) the evolution of all three matter components is identical.

As previously seen, the decoupling is a crucial point for structure formation, and it assumes a fundamental role specially in the mirror sector, where it occurs before than in the ordinary one: mirror baryons can start before growing perturbations in their density distribution. For this reason it's important to analyze the effect of changing the mirror decoupling time, obtained changing the value of x and leaving unchanged all other parameters, as it is possible to do using figures 12b, 15 and 16 for $x = 0.6, 0.5, 0.4, 0.3, 0.2$ and the same scale $\log k = -1.0$. It is evident the shift of the mirror decoupling toward lower values of a when reducing x , according to the law (8), which states a direct proportionality between the two. In particular, for $x < x_{\text{eq}} \approx 0.3$ mirror decoupling occurs before the horizon crossing of the perturbation, and mirror baryons mimic more and more the CDM, so that for $x \simeq 0.2$ the perturbations in the two components are indistinguishable. For the ordinary sector apparently there are no changes, but at a more careful inspection we observe some difference due to the different amount of relativistic mirror species (proportional to x^4), which slightly shifts the matter-radiation equality. This effect is more clear in figure 17, where we plot only the CDM and the ordinary baryons for the cases $x = 0.2$ and 0.6 : for the lower value of x there are less mirror photons, the MRE occurs before and the perturbation in the collisionless component starts growing before proportionally to the scale factor; thus, when the baryons decouple, their perturbation rapidly grows to equalize that in the CDM, which meanwhile has raised more for the lower x .

Obviously, these are cases where the CDM continues to be the dominant form of dark matter, and drives the growth of perturbations, given its continuous increase. In any case, if the dominant form of dark matter is made of mirror baryons the situation is practically the same, as visible comparing figures 15b and 18a (where we see only slight differences on the CDM and mirror baryons behaviours in the central region of the plots), since mirror baryons decouple before than ordinary ones and fall into the potential wells of the CDM, reinforcing them.

Finally, in the interesting case where mirror baryons constitute *all* the dark matter, they drive the evolution of perturbations. In fact, in figure 18b we clearly see that the density fluctuations start growing in the mirror matter and the visible baryons are involved later, after being recombined, when they rewrite the spectrum of already developed mirror structures. This is another effect of a mirror decoupling occurring earlier than the ordinary one: the mirror matter can drive the growth of perturbations in ordinary matter and provide the rapid growth soon after recombination necessary to take into account of the evolved structures that we see today.

After all the considerations made in this paper, it is evident that the case of mirror baryons is very interesting for structure formation, because they are collisional between themselves but collisionless for the ordinary sector, or, in other words, they are self-collisional. In this situation baryons and photons in the mirror sector are tightly coupled until decoupling, and structures cannot grow before this time, but the mirror decoupling happens before the ordinary one, thus structures have enough time to grow according to the limits imposed by CMB and LSS (something not possible in a purely ordinary baryonic scenario). Another important feature of the mirror dark matter scenario is that, if we consider small values of x , the evolution of primordial perturbations is very similar to the CDM case, but with a fundamental difference: there exist a cutoff scale due to the mirror Silk damping, which kills the small scales, overcoming the problems of the CDM scenario with the excessive number of small satellites. These are important motivations to go further in this work and investigate the effects of the mirror sector on the CMB and LSS power spectra, as we will do in Paper 2 [22].

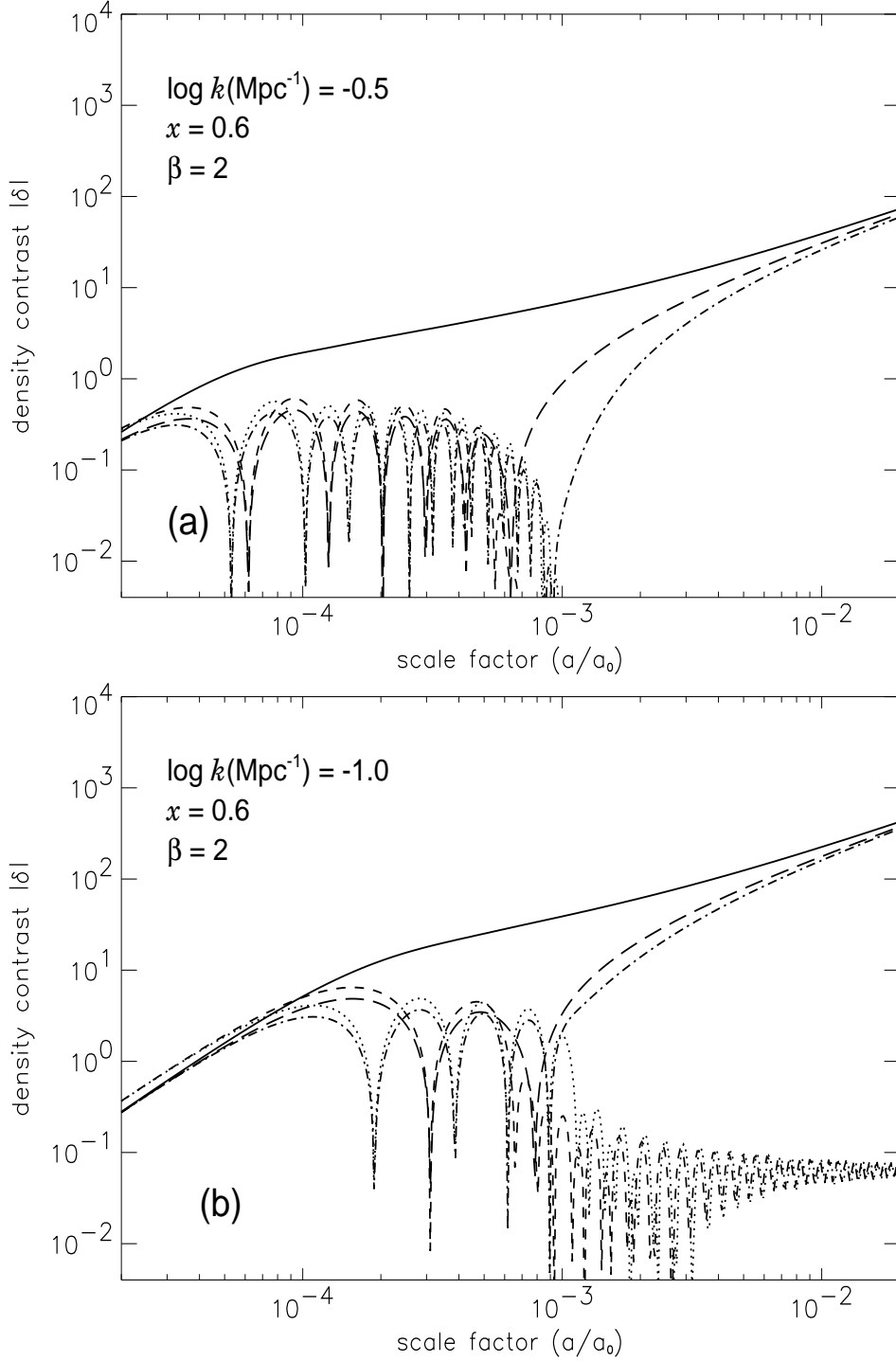


Figure 12: Evolution of perturbations for the components of a Mirror Universe: cold dark matter (solid line), ordinary baryons and photons (dot-dashed and dotted) and mirror baryons and photons (long dashed and dashed). The model is a flat Universe with $\Omega_m = 0.3$, $\Omega_b h^2 = 0.02$, $\Omega'_b h^2 = 0.04$ ($\beta = 2$), $h = 0.7$, $x = 0.6$, and plotted scales are $\log k(\text{Mpc}^{-1}) = -0.5$ (a) and -1.0 (b).

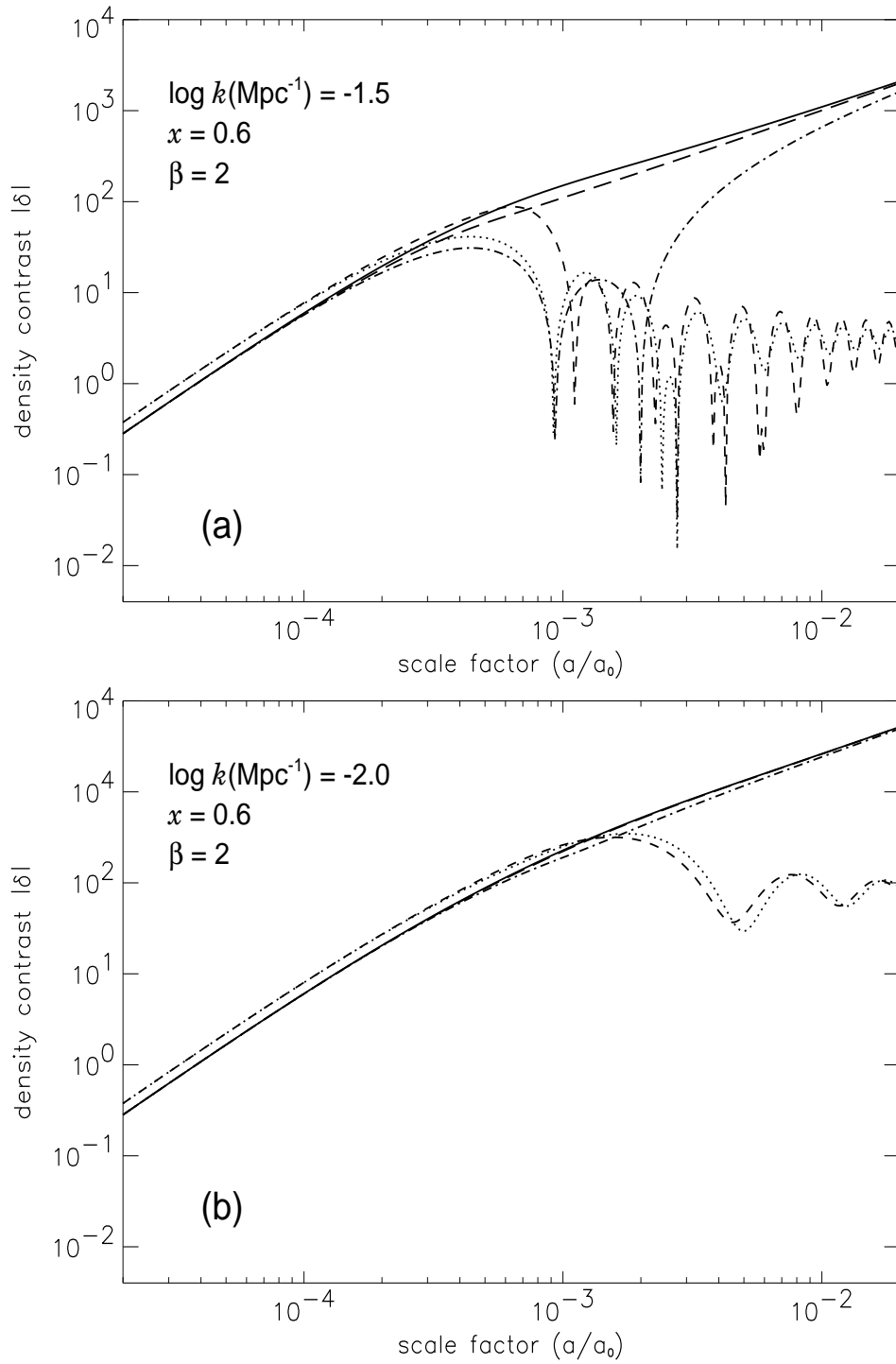


Figure 13: The same as in figure 12, but for scales $\log k(\text{Mpc}^{-1}) = -1.5$ (a) and -2.0 (b).

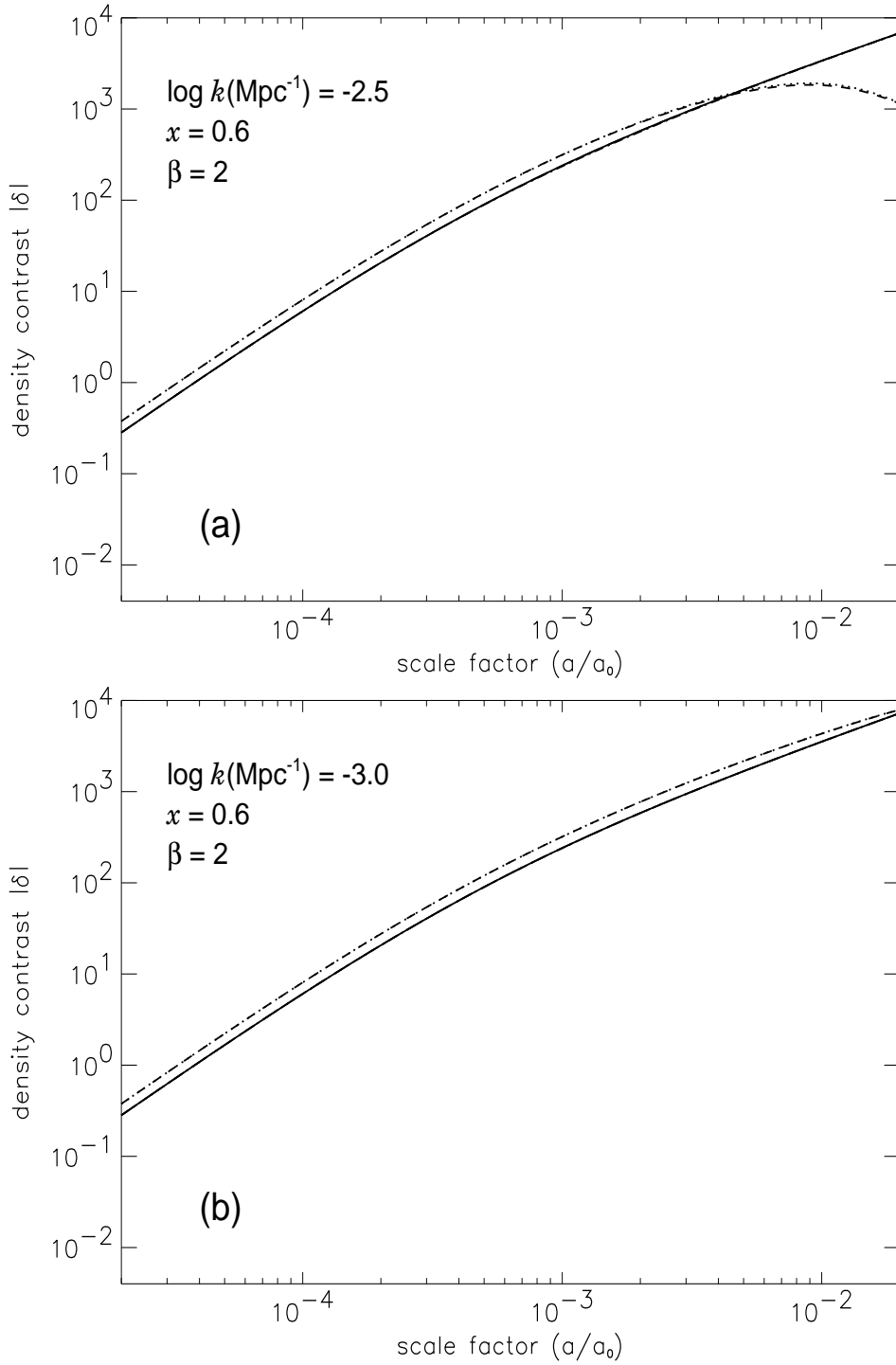


Figure 14: The same as in figure 12, but for scales $\log k(\text{Mpc}^{-1}) = -2.5$ (a) and -3.0 (b).

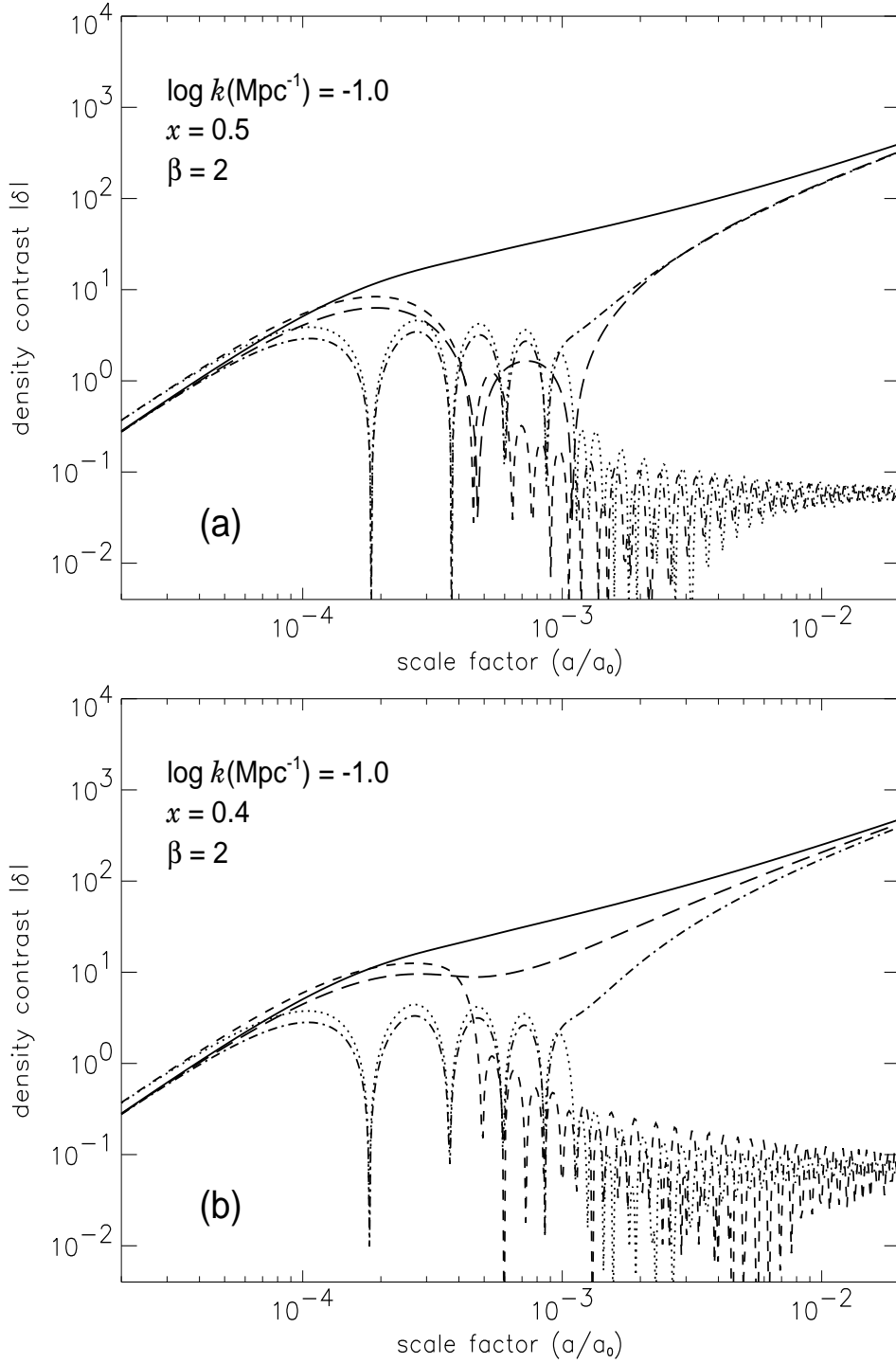


Figure 15: Evolution of perturbations for the components of a Mirror Universe: cold dark matter (solid line), ordinary baryons and photons (dot-dashed and dotted) and mirror baryons and photons (long dashed and dashed). The model is a flat Universe with $\Omega_m = 0.3$, $\Omega_b h^2 = 0.02$, $\Omega'_b h^2 = 0.04$ ($\beta = 2$), $h = 0.7$, $x = 0.5$ (a) or 0.4 (b), and plotted scale is $\log k(\text{Mpc}^{-1}) = -1.0$.

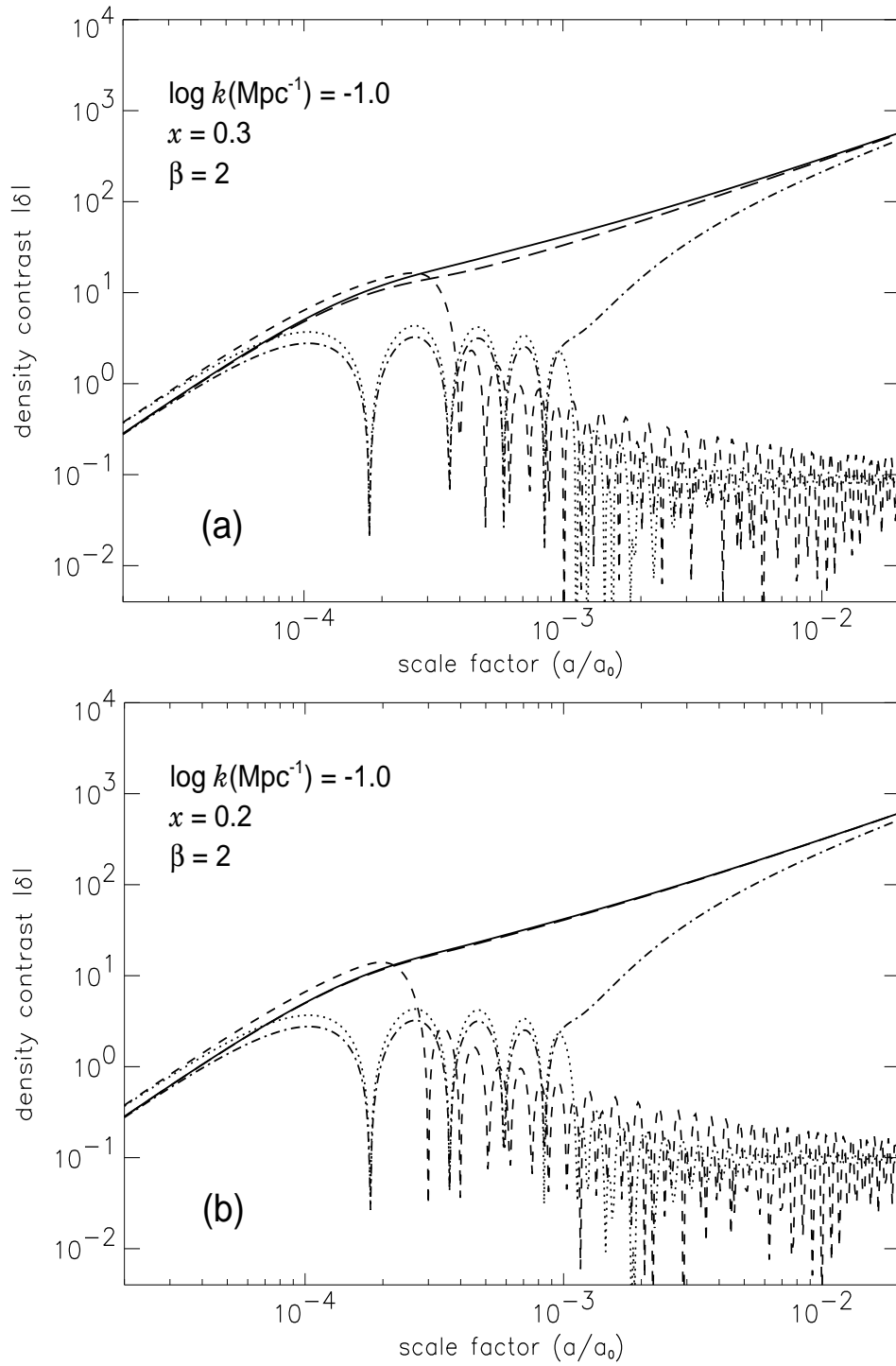


Figure 16: The same as in figure 15, but for $x = 0.3$ (a) and 0.2 (b).

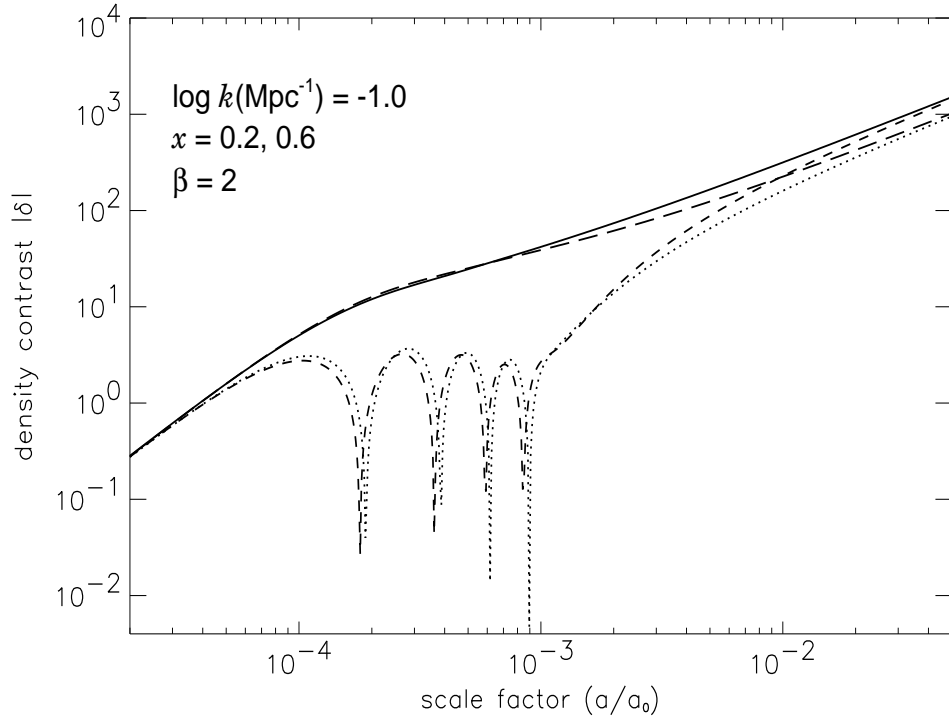


Figure 17: Evolution of perturbations in a Mirror Universe for cold dark matter (solid and long dashed lines) and ordinary baryons (dashed and dotted). The models are flat, with $\Omega_m = 0.3$, $\Omega_b h^2 = 0.02$, $\Omega'_b h^2 = 0.04$ ($\beta = 2$), $h = 0.7$, $x = 0.2$ (solid and dashed) and 0.6 (long dashed and dotted), and $\log k(\text{Mpc}^{-1}) = -1.0$. The highest scale factor plotted here is 0.05 , while in all other figures it is 0.02 .

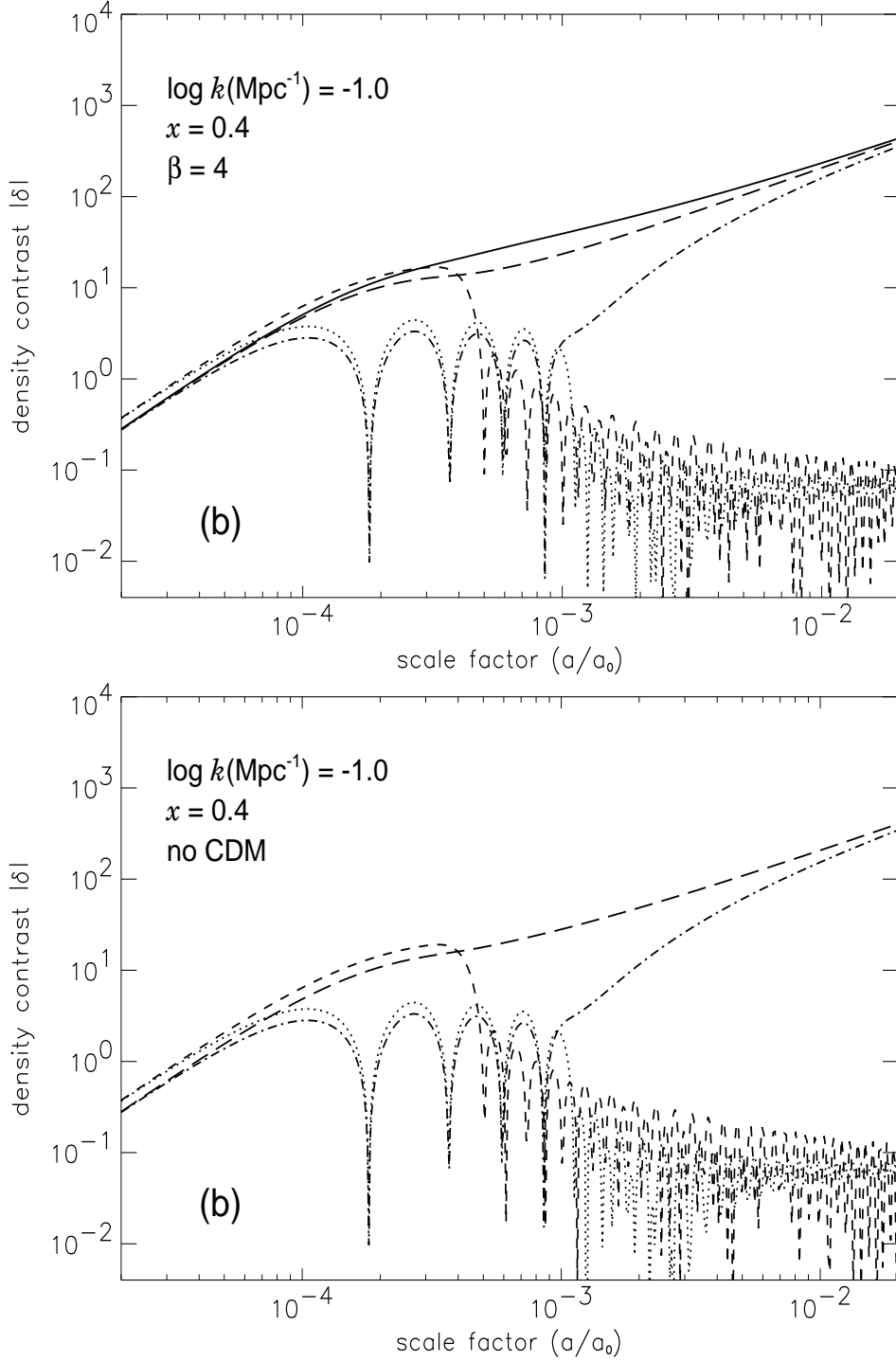


Figure 18: Evolution of perturbations for the components of a Mirror Universe: cold dark matter (solid line), ordinary baryons and photons (dot-dashed and dotted) and mirror baryons and photons (long dashed and dashed). The models are flat with $\Omega_m = 0.3$, $\Omega_b h^2 = 0.02$, $\Omega'_b = 4\Omega_b$ (a) or $(\Omega_m - \Omega_b)$ (no CDM) (b), $h = 0.7$, $x = 0.4$, and $\log k(\text{Mpc}^{-1}) = -1.0$.

6 Conclusions

We have studied the structure formation in linear regime for a Universe with mirror dark matter. We extended the Jeans theory to the more general case where the Universe is made of two sectors, ordinary and mirror, using a pre-existent bound (coming from the BBN limits) on the mirror temperature: in the relativistic expansion epoch the cosmological energy density is dominated by the ordinary component and the mirror one gives a negligible contribution, while for the non-relativistic epoch the complementary situation can occur when the mirror baryon matter density is bigger than the ordinary one, $\Omega'_b > \Omega_b$, and hence the mirror baryonic dark matter (MBDM) can contribute the dark matter of the Universe along with the CDM or even constitute a dominant dark matter component.

Since the existence of a mirror hidden sector changes the time of key epochs, there are important consequences on the structure formation scenario for a Mirror Universe. We studied this scenario in presence of adiabatic scalar density perturbations, which are at present the most probable kind of primordial fluctuations, in the context of the Jeans gravitational instability theory.

Given that the physics is the same in both sectors, key differences are the shifts of fundamental epochs, namely the baryon-photon equipartition and the matter-radiation decoupling occur in the mirror sector before than in the ordinary one: $a'_{b\gamma} < a_{b\gamma}$; $a'_{\text{dec}} < a_{\text{dec}}$. The first step was the study of the mirror sound speed and its comparison with the ordinary one and with the velocity dispersion of a typical cold dark matter candidate. From this study we obtained the mirror Jeans length and mass, again to be compared with the same quantities obtained for the ordinary sector and for the cold dark matter. There are two different possibilities, according to the value of x , which can be higher or lower than $x_{\text{eq}} \approx 0.046(\Omega_m h^2)^{-1}$, the value for which mirror decoupling occurs at matter-radiation equality time.

The values of the length and mass scales clearly depend on the mirror sector temperature and baryonic density, but we found that M'_J is always smaller than M_J , with a typical ratio ~ 50 for $x > x_{\text{eq}}$, while for cold dark matter it is several orders of magnitude lower. For $x < x_{\text{eq}}$, M'_J is few orders smaller than the same quantity obtained for the case $x > x_{\text{eq}}$.

Another important quantity to describe the structure evolution is the dissipative scale, represented in the mirror sector by the mirror Silk scale. We found that it is much lower than the ordinary one, obtaining $M'_S \sim 10^{10} M_\odot$ (around a typical galactic mass) for $x \simeq x_{\text{eq}}$, a value similar to the free streaming scale for a typical warm dark matter candidate, and much higher than the one for cold dark matter.

We collected all these informations in two different mirror scenarios, for $x > x_{\text{eq}}$ and $x < x_{\text{eq}}$. In the latter case we obtained a maximum mirror Jeans scale similar to the mirror Silk mass, so that practically all perturbations with masses greater than this Silk mass grow uninterruptedly, just as in a cold dark matter scenario.

After this, we modified a numerical code existing for the standard Universe in order to take into account a hidden mirror sector, and computed the evolution of perturbations in the linear regime for the components present in a Mirror Universe, namely the ordinary and mirror baryons and photons, and the cold dark matter. We did this for various mirror temperatures and baryon densities, and for different perturbative scales, finding all the features predicted by our structure formation study (as for example the mirror decoupling and the CDM-like behaviour for low x -values).

This was the first step in order to obtain the photon and matter power spectra for a Universe with mirror dark matter and compare them with observations, and this will be exactly the object of the next paper of this series.

Acknowledgements

I am grateful to my invaluable collaborators Zurab Berezhiani, Denis Comelli and Francesco Villante. I would like to thank also Silvio Bonometto, Stefano Borgani, Alfonso Cavaliere and Nicola Vittorio for interesting discussions.

References

- [1] R. Foot, H Lew and R. R. Volkas, Phys. Lett. B 272, 67 (1991).
The idea of mirror particles was earlier discussed in:
T. D. Lee and C. N. Yang, Phys. Rev. 104, 256 (1956);
I. Kobzarev, L. Okun and I. Pomeranchuk, Sov. J. Nucl. Phys. 3, 837 (1966);
M. Pavsic, Int. J. Theor. Phys. 9, 229 (1974).
For a review:
R. Foot, hep-ph/0207175;
R. Foot, *Shadowlands, quest for mirror matter in the Universe*, Universal Publishers, Parkland FL, 2002;
R. Foot, astro-ph/0407623;
Z. Berezhiani, hep-ph/0312335.
- [2] S. I. Blinnikov and M. Yu. Khlopov, Sov. J. Nucl. Phys. 36, 472 (1982);
S. I. Blinnikov and M. Yu. Khlopov, Sov. Astron. 27, 371 (1983).
- [3] A. Yu. Ignatiev and R. R. Volkas, Phys. Rev. D 68, 023518 (2003) [hep-ph/0304260].
- [4] Z. Berezhiani, P. Ciarcelluti, D. Comelli and F. L. Villante, astro-ph/0312605;
P. Ciarcelluti, astro-ph/0312607;
P. Ciarcelluti, astro-ph/0409629.
- [5] R.N. Mohapatra, V. Teplitz, Astrophys. J. 478, 29 (1997) [astro-ph/9603049];
R.N. Mohapatra, V. Teplitz, Phys. Rev. D 62, 063506 (2000) [astro-ph/0001362];
R. Foot and R. R. Volkas, astro-ph/0407522.
- [6] S. Blinnikov, astro-ph/9801015;
R. Foot, Phys. Lett. B 452, 83 (1999) [astro-ph/9902065];
R.N. Mohapatra, V. Teplitz, Phys. Lett. B 462, 302 (1999) [astro-ph/9902085].
- [7] S. Blinnikov, astro-ph/9902305;
R. Volkas, Y. Wong, Astropart. Phys. 13, 21 (2000) [astro-ph/9907161];
R.N. Mohapatra, S. Nussinov and V.L. Teplitz, Astropart. Phys. 13, 295 (2000) [astro-ph/9909376];
S. Blinnikov, Surveys High Energ. Phys. 15, 37 (2000) [astro-ph/9911138];
R. Foot and Z. K. Silagadze, astro-ph/0404515.
- [8] Z. Berezhiani, L. Gianfagna and M. Giannotti, Phys. Lett. B 500 (2001) 286 [hep-ph/0009290];
L. Gianfagna, M. Giannotti and F. Nesti, hep-ph/0409185.
- [9] S. L. Glashow, Phys. Lett. B 167, 35 (1986);
R. Foot and S. N. Gninenko, Phys. Lett. B 480, 171 (2000) [hep-ph/0003278];
R. Foot, astro-ph/0309330;
S.N. Gninenko, Phys. Lett. B 326 (1994) 317.

- [10] A. Badertscher *et al.*, hep-ex/0311031.
- [11] R. Foot, Phys. Rev. D 69, 036001 (2004) [hep-ph/0308254];
 R. Foot, astro-ph/0403043;
 R. Foot, Mod. Phys. Lett. A 19, 1841 (2004) [astro-ph/0405362].
- [12] A. Yu. Ignatiev and R. R. Volkas, Phys. Rev. D 62, 023508 (2000) [hep-ph/0005125];
 Z. K. Silagadze, Acta Phys. Pol. B 32, 99 (2001) [hep-ph/0002255];
 R. Foot, Acta Phys. Polon. B 32, 3133 (2001) [hep-ph/0107132];
 R. Foot and T. L. Yoon, Acta Phys. Polon. 33, 1979 (2002) [astro-ph/0203152];
 R. Foot and S. Mitra, Astropart. Phys. 19, 739 (2003) [astro-ph/0211067];
 A. Yu. Ignatiev and R. R. Volkas, hep-ph/0306120;
 R. Foot and S. Mitra, Phys. Rev. D 68, 071901 (2003) [hep-ph/0306228];
 Z. K. Silagadze, astro-ph/0311337.
- [13] S. Mitra and R. Foot, Phys. Lett. B 558, 9 (2003) [astro-ph/0301229];
 R. Foot and S. Mitra, Phys. Lett. A 315, 178 (2003) [cond-mat/0306561].
- [14] R. Foot, Phys. Lett. B 471, 191 (1999) [astro-ph/9908276];
 R. Foot, Phys. Lett. B 505, 1 (2001) [astro-ph/0101055];
 R. Foot and Z. K. Silagadze, Acta Phys. Pol. B 32, 2271 (2001) [astro-ph/0104251];
 R. Foot, A. Yu. Ignatiev and R. R. Volkas, Astropart. Phys. 17, 195 (2002) [astro-ph/0010502];
 Z. K. Silagadze, Acta Phys. Pol. B 33, 1325 (2002) [astro-ph/0110161];
 R. Foot, astro-ph/0406257.
- [15] R. Foot and R. R. Volkas, Phys. Lett. B 517, 13 (2001) [hep-ph/0108051].
- [16] Z. Berezhiani, Acta Phys. Polon. B 27 (1996) 1503;
 R. Foot, H. Lew and R. R. Volkas, JHEP 007, 032 (2000) [hep-ph/0006027];
 R. N. Mohapatra, S. Nussinov and V. L. Teplitz, Phys. Rev. D 66, 063002 (2002) [hep-ph/0111381].
- [17] B. Holdom, Phys. Lett. B 166, 196 (1986);
 E. Carlson and S. Glashow, Phys. Lett. B193, 168 (1987);
 R. Foot and X-G. He, Phys. Lett. B 267, 509 (1991);
 M. Collie and R. Foot, Phys. Lett. B 432, 134 (1998) [hep-ph/9803261];
 A. Yu. Ignatiev and R. R. Volkas, Phys. Lett. B 487, 294 (2000) [hep-ph/0005238];
 R. Foot, A. Yu. Ignatiev and R. R. Volkas, Phys. Lett. B 503, 355 (2001) [astro-ph/0011156].
- [18] E. Akhmedov, Z. Berezhiani and G. Senjanović, Phys. Rev. Lett. 69, 3013 (1992);
 R. Foot, Mod. Phys. Lett. A 9, 169 (1994) [hep-ph/9402241];
 R. Foot and R. R. Volkas, Phys. Rev. D 52, 6595 (1995) [hep-ph/9505359];
 Z. Berezhiani, R.N. Mohapatra, Phys. Rev. D 52, 6607 (1995) [hep-ph/9505385];
 Z. Silagadze, Phys. Atom. Nucl. 60, 272 (1997) [hep-ph/9503481];
 R. Foot, R.R. Volkas, Phys. Rev. D 61, 043507 (2000) [hep-ph/9904336];
 V. Berezhinsky, M. Narayan, F. Vissani, Nucl. Phys. B 658, 254 (2003) [hep-ph/0210204].
- [19] Z. Berezhiani, D. Comelli and F. L. Villante, Phys. Lett. B 503, 362 (2001) [hep-ph/0008105].

- [20] E. W. Kolb, D. Seckel and M. S. Turner, *Nature* 314, 415 (1985);
H. M. Hodges, *Phys. Rev. D* 47, 456 (1993);
Z. G. Berezhiani, A. D. Dolgov and R. N. Mohapatra, *Phys. Lett. B* 375, 26 (1996) [hep-ph/9511221];
V. Berezhinsky and A. Vilenkin, *Phys. Rev. D* 62, 083512 (2000) [hep-ph/9908257].
- [21] L. Bento and Z. Berezhiani, *Phys. Rev. Lett.* 87, 231304 (2001) [hep-ph/0107281];
L. Bento and Z. Berezhiani, hep-ph/0111116;
L. Bento and Z. Berezhiani, *Fortsch. Phys.* 50 (2002) 489;
R. Foot and R. R. Volkas, *Phys. Rev. D* 68, 021304 (2003) [hep-ph/0304261];
R. Foot and R. R. Volkas, *Phys. Rev. D* 69, 123510 (2004) [hep-ph/0402267].
- [22] P. Ciarcelluti, astro-ph/0409633.
- [23] D.N. Spergel *et al.*, *Astrophys. J. Suppl.* 148, 175 (2003) (astro-ph/0302209).
- [24] T. Padmanabhan, *Structure Formation in the Universe*, Cambridge University Press (1993).
- [25] C.G. Tsagas, *Lecture Notes in Physics* 592, 223 (2002) [astro-ph/0201405].
- [26] Y.B. Zeldovich, *Soviet Phys. Usp.* 9, 602 (1967).
- [27] K. Enqvist, H. Kurki-Suonio, J. Valiviita, *Phys. Rev. D* 62, 103003 (2000) [astro-ph/0006429];
K. Enqvist, H. Kurki-Suonio, J. Valiviita, *Phys. Rev. D* 65, 043002 (2002) [astro-ph/0108422].
- [28] J. Jeans, *Phil. Trans.* 199A, 49 (1902);
J. Jeans, *Astronomy and Cosmology*, Cambridge University Press (1928).
- [29] J. Silk, *Nature* 215, 1155 (1967).
- [30] E.W. Kolb & M.S. Turner, *The Early Universe*, Addison-Wesley (1990).
- [31] C. Ma & E. Bertschinger, *Astrophys. J.* 455, 7 (1995) [astro-ph/9506072].